



TECHNISCHE  
UNIVERSITÄT  
WIEN

Vienna University of Technology

## DIPLOMARBEIT

### **Software Module for Automated Thermoluminescence Dating**

Ausgeführt am

ATOMINSTITUT

der Technischen Universität Wien

unter Anleitung von

UNIV.PROF. DIPL.-ING. DR. TECHN. NORBERT VANA

und

UNIV.ASS. DIPL.-ING. DR. TECHN. MICHAEL HAJEK

durch

PETULA BLAMAUER  
Markt 46  
3074 Michelbach

Wien am, \_\_\_\_\_

## **Declaration**

I declare that this thesis is my own work and has not been submitted in any form for another degree or diploma at any university or other institution of tertiary education. Information arrived from the published or unpublished work of others has been acknowledged in the text and a list of references is given.

Vienna,

Petula Blamauer

## Acknowledgements

I would like to thank my advisor, Univ.Prof. Dipl.-Ing. Dr.techn. Norbert Vana, who made it possible to write this thesis.

With all my heart I would like to thank Dipl.-Ing. Robert Bergmann, ADir. Ing. Manfred Fugger, Univ.Ass. Dipl.-Ing. Dr.techn. Michael Hajek and Dipl.-Ing. Dr. Johannes Sterba of the Institute of Atomic and Subatomic Physics of Vienna University of Technology for giving me all the support and freedom I needed and also taking the time for explanations and discussing results.

I would also like to express my gratitude to Dipl.-Ing. Dr.techn. Wolfgang Gratzl for his constructive criticism and support throughout this project.

Especially, I would like to thank my family: my parents and my brother whose love, help and support have made my academic studies as well as writing this thesis possible.

Petula Blamauer

## **Kurzfassung**

Thermolumineszenz ist eine wichtige Methode zur Altersbestimmung von Ziegeln, Tonfragmenten und Keramiken. Das Hauptaugenmerk dieser Arbeit liegt auf der Altersbestimmung von Proben aus Alkoven (Oberösterreich) und Petronell-Carnuntum (Niederösterreich). Das Alter wird mittels der Feinkorn-technik ermittelt.

Die Berechnung des Alters erfolgt über ein Softwaremodul, das im Rahmen dieser Diplomarbeit erneuert und verbessert wurde.

## **Abstract**

Thermoluminescence is an important tool for the age determination of bricks, clay fragments and diverse ceramics.

The focus of this work lies on the age determination of samples from Alkoven (Upper Austria) and Petronell-Carnuntum (Lower Austria). The age is obtained by the fine-grain technique.

The calculation itself is carried out by a software module which was renewed and enhanced throughout this thesis.



# Contents

<b>1</b>	<b>Introduction</b>	<b>1</b>
<b>2</b>	<b>Theoretical Foundations</b>	<b>2</b>
2.1	Luminescence	2
2.2	Principle of Luminescence Dating	2
2.3	Thermoluminescence Dating	4
2.3.1	Energy-Band Model	4
2.4	Thermoluminescence Glow-Curves	5
2.5	Effects Affecting Thermoluminescence Dating	9
2.5.1	Anomalous Fading	9
2.5.2	Bleaching	10
2.5.3	Spurious Thermoluminescence	10
2.5.4	Thermal Instability	11
2.5.5	Thermal Quenching	11
2.6	Plateau Test	11
2.7	Determination of the Paleodose Using the Additive Method	13
2.8	Fine-Grain Dating	14
2.9	Age Calculation	16
2.9.1	$\alpha$ -Efficiency	17
2.9.2	$\alpha$ -Dose Rate	18
2.9.3	$\beta$ -Dose Rate	19
2.9.4	$\gamma$ -Dose Rate	20
2.9.5	Cosmic Dose Rate	22
2.10	Error Estimation	23
2.10.1	Statistical (Random) Errors	24
2.10.2	Systematic Errors	25
<b>3</b>	<b>Experiment Preparation and Execution</b>	<b>27</b>
3.1	Parameters of Age Determination	27
3.1.1	Thorium/Uranium-Ratio	27
3.1.2	Wetness Corrections	28
3.1.3	Determination of Potassium Concentration by Neutron Activation Analysis	29
3.1.4	External $\gamma$ -Dose Rate and Cosmic Dose Rate	33
3.2	Sample Preparation	34
3.2.1	Preparation	34
3.2.2	Drilling	34
3.2.3	Grinding	35
3.2.4	Fractionation	35

3.2.5	Sedimentation . . . . .	37
3.3	Measurement . . . . .	37
3.3.1	HVK-Device . . . . .	37
3.3.2	Measuring Sequence . . . . .	38
3.3.3	Age Calculation-Program Module . . . . .	44
<b>4</b>	<b>Results of Thermoluminescence Age Determination</b>	<b>68</b>
4.1	Sample from Alkoven, “PBP1” . . . . .	68
4.2	Sample from Petronell-Carnuntum, “PBP2” . . . . .	77
<b>5</b>	<b>Conclusion</b>	<b>82</b>
5.1	Sample of Alkoven, “PBP1” . . . . .	82
5.2	Sample of Petronell-Carnuntum, “PBP2” . . . . .	83
<b>A</b>	<b>Printout of Sample “PBP2”</b>	<b>84</b>

## List of Figures

2.1	Fluorescence and phosphorescence (Chen and McKeever, 1997) [1]	3
2.2	Energy-Band Model (Aitken, 1985) [2]	4
2.3	Thermoluminescence glow-curve; the dark area is the black body radiation determined by heating the sample a second time without any additional radiation. (Bøtter-Jensen 1998) [3]	6
2.4	Example of a glow-curve	7
2.5	Anomalous fading of a brick; (a) glow-curve of the immediately irradiated and measured sample; (b) glow-curve of the sample which was stored for 15 hours at -18 °C after irradiation and then measured; (Aitken, 1985) [2]	9
2.6	Bleaching of a limestone sample; (a) natural glow-curve unbleached; (b) after bleaching for 4 min; (c) after bleaching for 80 h; adapted from Bruce et al. (1999) [4]	10
2.7	Plateau test; (a) natural and artificial irradiated glow-curves; (b) ratios of the glow-curves;	12
2.8	The additive method (Aitken, 1998) [5]	13
2.9	Supra-linearity correction in second-glows (Aitken, 1985) [2]	14
2.10	Determination of the paleodose considering the intercept (Aitken, 1985) [2]	15
2.11	Supra- and sub-linearity (Aitken, 1985) [2]	15
3.1	$\alpha$ -counting system	27
3.2	$^{42}\text{K}$ peak of PBP2 in $\gamma$ -spectroscopy after neutron activation analysis	30
3.3	Analysis sheet of sample PBP2	32
3.4	Parameters in equation (3.9) by Prescott and Stephan (1982) [6]	33
3.5	Drilling under red light, desk space for drilling and ultrasonic bath	35
3.6	Desk space for fractionating, oven	36
3.7	HVK-device, device controlling computer (left) and data analyzing computer (right)	38
3.8	Schematic diagram of the HVK (Tatlisu, 1999) [7], opened HVK-device	39
3.9	Natural glow-curve	41
3.10	Natural and artificially $\beta$ -irradiated glow-curves	42
3.11	Plateau test	42
3.12	Zoomed integration interval	43
3.13	Regression lines	43
3.14	Age Calculation dialog	45
3.15	Alpha-Counting Rate dialog; sample PBP2	53
3.16	Background dialog; sample PBP2	56

3.17	Saturation Fraction/Saturation Weight Increase dialog; sample PBP2	58
3.18	Potassium Oxide-Contents dialog; standard SO-1 with sample PBP2	59
3.19	External $\gamma$ -Dose Rate; sample PBP2 . . . . .	61
3.20	Cosmic Dose Rate dialog; sample PBP2 . . . . .	63
3.21	Error Caused by Stony Surroundings dialog; sample PBP2 . . . . .	66
4.1	Sample “PBP1”; coated aluminium discs . . . . .	68
4.2	Natural and $\alpha$ -irradiated glow-curves of sample “PBP1” - original software . . . . .	69
4.3	Natural and $\alpha$ -irradiated glow-curves of sample “PBP1” - revised software . . . . .	69
4.4	Natural and $\beta$ -irradiated glow-curves of sample “PBP1” - original software . . . . .	70
4.5	Natural and $\beta$ -irradiated glow-curves of sample “PBP1” - revised software . . . . .	70
4.6	Second-glow-curves of sample “PBP1” - original software . . . . .	71
4.7	Second-glow-curves of sample “PBP1” - revised software . . . . .	71
4.8	Plateau test of sample “PBP1” - original software . . . . .	72
4.9	Plateau test with zoomed integration interval (276-304 °C) of sample “PBP1” - original software . . . . .	72
4.10	Plateau of sample “PBP1” - revised software . . . . .	73
4.11	Plateau test with zoomed integration interval (276-304 °C) of sample “PBP1” - revised software . . . . .	73
4.12	Regression lines of sample “PBP1” - original software . . . . .	74
4.13	Regression lines of sample “PBP1” - revised software . . . . .	74
4.14	Age Calculation of sample “PBP1” - original software . . . . .	75
4.15	Age Calculation of sample “PBP1” - revised software . . . . .	75
4.16	Sample “PBP2”; coated aluminium discs . . . . .	77
4.17	Natural and $\alpha$ -irradiated glow-curves of sample “PBP2” . . . . .	78
4.18	Natural and $\beta$ -irradiated glow-curves of sample “PBP2” . . . . .	78
4.19	Second-glow-curves of sample “PBP2” . . . . .	79
4.20	Plateau of sample “PBP2” . . . . .	79
4.21	Plateau test with zoomed integration interval (270-300 °C) of sample “PBP2” . . . . .	80
4.22	Regression lines of sample “PBP2” . . . . .	80
4.23	Age Calculation of sample “PBP2” . . . . .	81
A.1	Printout of sample “PBP2”, page 1 . . . . .	84
A.2	Printout of sample “PBP2”, page 2 . . . . .	85

## Listings

1	Procedure <i>CalcAge</i> manages the calculation of the age of the sample along with the occurring errors basing upon the formulas in the sections 2.9 and 2.10. . . . .	48
2	Procedure <i>ButtonAgeParametersSaveClick</i> for saving parameters .	52
3	Procedure <i>ButtonAgeParametersLoadClick</i> for loading parameters	52
4	Procedure <i>ButtonaCCalculateClick</i> manages the calculation of the $\alpha$ -counting rate and pairs rate . . . . .	55
5	Procedure <i>ButtonBGCalculateClick</i> manages the calculation of the background value . . . . .	57
6	Procedure <i>ButtonK2OCalculateClick</i> manages the calculation of the potassium and potassium oxide-concentrations within the sample	61
7	Procedure <i>ButtonDgExtCalculateClick</i> manages the calculation of the corrected $\gamma$ -dose rate . . . . .	62
8	Procedure <i>ButtonLCalculateClick</i> manages the calculation of the geomagnetic latitude . . . . .	64
9	Procedure <i>ButtonDkCalculateClick</i> manages the calculation of the cosmic dose rate . . . . .	65
10	Procedure <i>ButtonSigma3CalculateClick</i> manages the calculation of error caused by stony surroundings . . . . .	66

# 1 Introduction

Thermoluminescence is a well established technique in archeological dating and dosimetry. Over the years, energy is stored in minerals due to ionizing radiation. Measuring this energy which was absorbed by a sample in this time is the basic principle of thermoluminescence dating. The sample is heated and thereby releases this energy by emitting light.

The main task of this thesis was the age determination of two samples, a brick from Alkoven in Upper Austria and a broken fragment from Petronell-Carnuntum in Lower Austria. The fine-grain technique shall be used for both samples.

The other assignment was to revise a part of the dating software used for the age determination of samples at the Institute of Atomic and Subatomic Physics of Vienna University of Technology due to compatibility problems with modern computer systems. Several features have been added and the user-friendliness was improved.

In chapter 2 the principle of luminescence is described along with important terms and definitions such as glow-curve, special effects which might influence thermoluminescence dating, plateau test, fine-grain dating etc. Furthermore, the determination of the paleodose and the calculations needed for age determination including error estimations are explained.

Chapter 3 overviews the determination of additionally needed parameters and the used experimental setups. Moreover, the processes of sample preparation, artificial irradiation with  $\alpha$ -or  $\beta$ -sources, preheating and measurement are described.

The new software module is explained in detail.

In chapter 4 the results of measuring the two samples can be found. The revised software is compared to the original one.

## 2 Theoretical Foundations

### 2.1 Luminescence

Luminescence is the emission of light when an electron of an excited higher state returns to an unoccupied lower state following the previous absorption of energy. It is also known as "cold" light due to its usual occurrence at comparatively low temperatures and in addition to black body radiation. Luminescence therefore takes place after a physical system is supplied with energy which is absorbed in non-conducting crystalline materials and subsequently stored as potential energy. This energy can be provided by biochemical energy, chemical processes, beams of electrons, electrical fields, mechanical processes, ionizing radiation, optical or ultra-violet light, sound waves or heat.

Depending on the extent of the lag between the absorption of energy and the emission of light there are two phenomena: fluorescence where the characteristic time  $\tau_c$  is less than  $10^{-8}s$  and phosphorescence where  $\tau_c$  is more than  $10^{-8}s$ . Fluorescence describes spontaneous emissions whereas phosphorescence can be further divided into two parts. A precise description can be found at McKeever (1985) [8].

In Fig. 2.1 both phenomena are shown. Fluorescence on the left, where the transition from the short lasting excited state E to the ground state G can be seen. It can be delayed for a few milliseconds if the transition is spin or parity forbidden. Phosphorescence, which is shown on the right side, takes place when electrons from state E descend to a metastable state M. If the direct transition from M to G is forbidden the electrons have to be excited to state E first before they can return to the ground state. If the energy for this process is not available, the return to the ground state will be delayed (Chen and McKeever, 1997) [1].

### 2.2 Principle of Luminescence Dating

In order to use luminescence for dating the used ceramics have to be able to absorb and store the energy which is supplied. Most ceramics consist of crystalline materials such as quartz or feldspar. The lattice of these crystals can include defects and electrons are trapped due to these defects. Luminescence light is not emitted until these electrons are released by external stimulation such as heat or light.

The luminescence signal can be zeroed thermally by baking the ceramic for example. This means that this newly originated ceramic is "0 years old". After

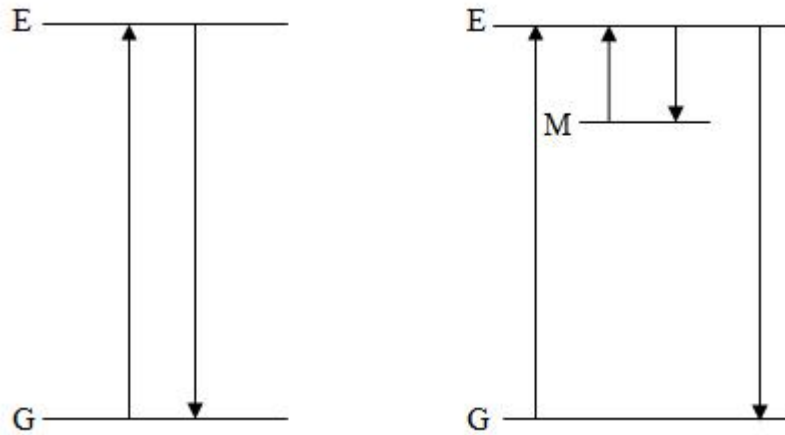


Figure 2.1: Fluorescence and phosphorescence (Chen and McKeever, 1997) [1]

that the signal starts to rebuild due to absorption of ionizing radiation from within the ceramic (uranium, thorium, potassium, rubidium) or from external radiation like cosmic or terrestrial radiation. If the ceramic is buried, it is shielded from high temperature and light.

In order to obtain the natural luminescence a fragment of the ceramic is extracted and afterwards exposed to heat. By irradiating the sample with a known dose and subsequent heating the sample's sensitivity to ionizing radiation can be determined.

The paleodose, which is the dose that is stored in the sample, can be obtained by comparison of the naturally and artificially irradiated results by help of luminescence measurements. The annual dose rate is determined by (radio) chemical analyses of the sample or can be measured directly at the place of burial. Hence the luminescence age is given by

$$Age[a] = \frac{P}{\dot{D}} \quad (2.1)$$

$P$ .....paleodose [Gy/a]

$\dot{D}$ ....annual dose rate [Gy/a]

where it has to be kept in mind that the age is based upon the last time the ceramic was heated adequately so that the natural luminescence was deleted (e.g. baking as mentioned above).



## 2.3 Thermoluminescence Dating

Thermally stimulated luminescence is the emission of light after a crystalline material has been excited and thereafter heated. It can occur because solids can absorb energy and store it for an adequately long period of time.

Techniques and methods of thermoluminescence dating can be found at Aitken (1985) [2].

### 2.3.1 Energy-Band Model

The energy-band model is consulted for describing the principle functionality of thermoluminescence whereas the valence band, the highest range of ground-state electron energies, and the conduction band, the range of energies higher than that of the valence band at nearly absolute zero, are used. Quartz and feldspar are insulators, so they have only these two bands with an energy gap in between. This gap is usually too broad so as to transfer the electrons from the valence band to the conduction band by thermal excitation at room temperature.

As real crystals vary from the ideal ones, defects occur in the lattice. They can be one-, two- or three-dimensional. Because of these defects or incorporated impurities metastable states, so-called “traps”, are generated within the energy gap.

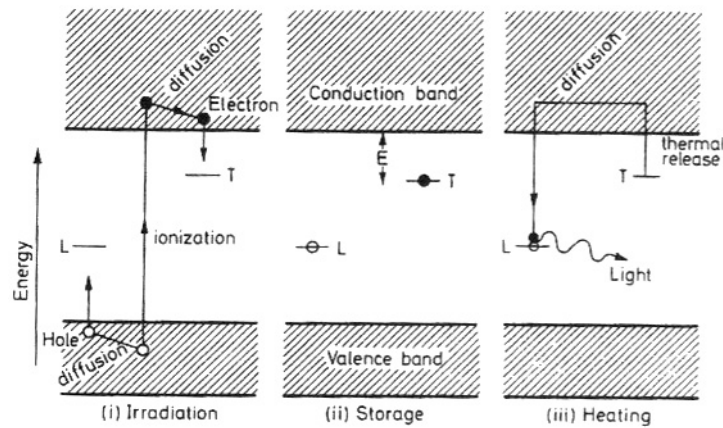


Figure 2.2: Energy-Band Model (Aitken, 1985) [2]

Fig. 2.2 shows the different stages of thermoluminescence. Through ionizing radiation electrons are excited and will either return directly to the ground state, or find an unoccupied recombination center or be trapped after passing the conduction band (Fig. 2.2 - Irradiation). The depths of the traps are an indicator for

their effectiveness (Fig. 2.2 - Storage). If they are too small, electrons might be released because of lattice vibrations that can occur during the whole lifetime of the ceramic. This eviction can be rushed by increasing the temperature. Hence the lifetime of the electrons is determined by the depth of the traps, the temperature and the frequency factor (attempt-to-escape frequency), and as a result the probability of the release of an electron from a trap and its transition to the conduction band is given by

$$p = \tau^{-1} = s \cdot e^{-\frac{E}{k_B \cdot T}} \quad (2.2)$$

$p$ .....transition probability [ $s^{-1}$ ]

$\tau$ .....lifetime [s]

$s$ .....attempt-to-escape frequency, relating to the vibration of the lattice [ $s^{-1}$ ]

$E$ .....trap depth [eV]

$k_B$ ...Boltzmann constant;  $k_B = 8.617343(15) \cdot 10^{-5} \frac{eV}{K}$  (Mohr et al., 2008) [9]

$T$ .....temperature [K]

and its value varies between  $10^9 s^{-1}$  and  $10^{16} s^{-1}$ . Therefore, electrons can be stored for a long time in these traps if the energy difference between conduction band and trap is large enough. But as mentioned above it is possible to release the electrons by increasing the temperature (Fig. 2.2 - Heating). The deeper the trap the more heat is necessary to empty it. The electrons can then be lifted into the conduction band and are able to reach empty recombination centers while emitting light.

## 2.4 Thermoluminescence Glow-Curves

Plotting the amount of emitted light over the heating temperature of the sample gives the glow-curve. Fig. 2.3 shows an example where the different peaks occur due to the different depths of the traps. Electrons are released from these traps at characteristic temperatures.

Different assumptions and formulas for obtaining the luminescence intensity are discussed by McKeever and Chen (1997) [10]. A detailed analysis of glow-curves can be found at Basun et al. (2003) [11].

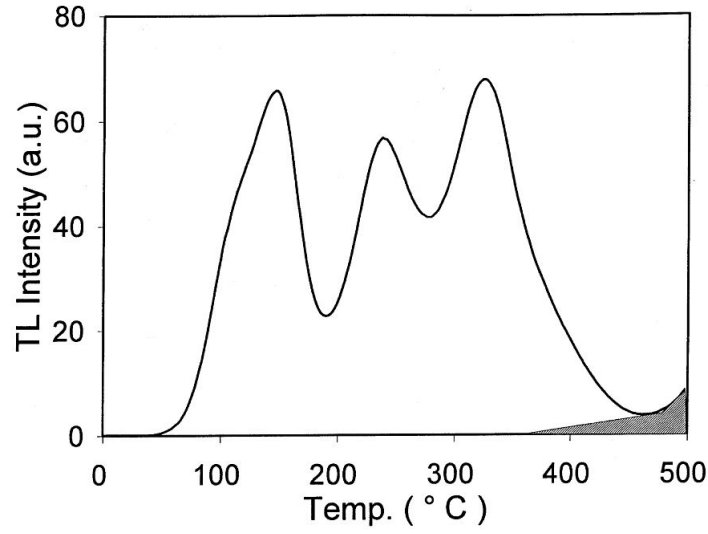


Figure 2.3: Thermoluminescence glow-curve; the dark area is the black body radiation determined by heating the sample a second time without any additional radiation. (Bøtter-Jensen 1998) [3]

### First Order Kinetics

Compared to recombination the process of retrapping can be neglected and therefore the time rate of change of the trap population density is given by (McKeever and Chen, 1997) [10]

$$\frac{dn}{dt} = -p \cdot n(t) = -n(t) \cdot s \cdot e^{-\frac{E}{k_B \cdot T}} \quad (2.3)$$

$n$ .....amount of electrons in traps

$p$ .....transition probability [ $s^{-1}$ ]

$s$ .....attempt-to-escape frequency, relating to the vibration of the lattice [ $s^{-1}$ ]

$E$ .....trap depth [eV]

$k_B$ ...Boltzmann constant;  $k_B = 8.617385 \cdot 10^{-5}$  [eV/K]

$T$ .....temperature [K]

and by integration from  $t=0$  to  $T$  using a constant heating rate  $\beta = \frac{dT}{dt}$  the luminescence intensity considering

$$\frac{dn}{dt} = -p \cdot n(t) \Rightarrow n(t) = n_0 \cdot e^{-\int p dt} = n_0 \cdot e^{-\int s \cdot e^{-\frac{E}{k_B \cdot T}} dt} \quad (2.4)$$

can be written as

$$I(T) = -\frac{dn}{dt} = n_0 \cdot s \cdot e^{-\frac{E}{k_B \cdot T}} e^{-\frac{s}{\beta} \int_{T_0}^T e^{-\frac{E}{k_B \cdot \tau}} d\tau}. \quad (2.5)$$

$n_0$ ...amount of electrons in traps at  $t=0$

$\beta$ ....heating rate

$T_0$ ...lower value of temperature

This expression usually gives a good description of the first stage of the peak but might differ at later stages. The peak position is obtained by assuming the possibility that an electron is released and by considering the amount of electrons still in the traps. Representative for this order of kinetics is the asymmetric shape of the thermoluminescence glow-curve. At lower temperatures the curve shows a flatter increase whereas at high temperatures a sharp decline can be observed.

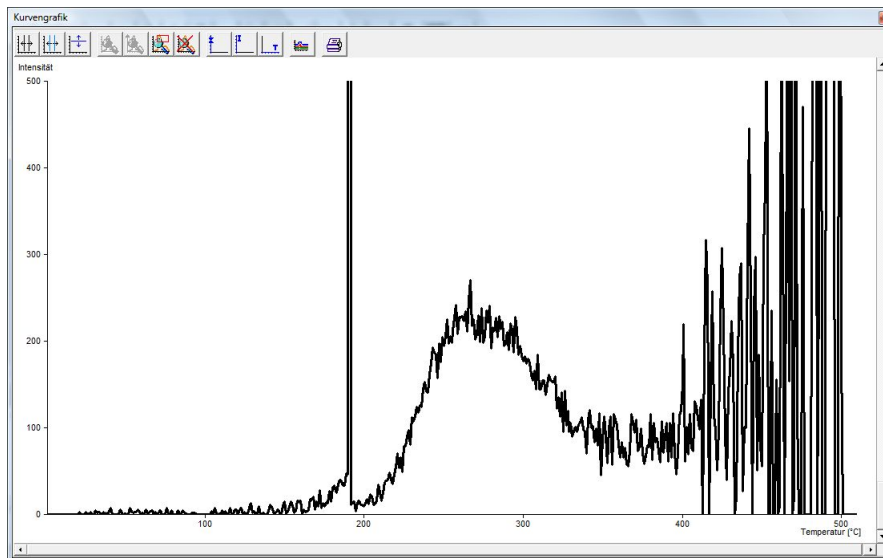


Figure 2.4: Example of a glow-curve

## Second Order Kinetics

The assumption made here is that retrapping contributes to the process and

therefore the time rate of change of the trap population density is given by (Basun et al., 2003) [11]

$$\frac{dn}{dt} = -n^2 \cdot \frac{s}{N} \cdot e^{-\frac{E}{k_B \cdot T}} \quad (2.6)$$

N...amount of traps

and the luminescence intensity results in

$$I(T) = -\frac{dn}{dt} = n_0^2 \cdot \frac{s}{N} \cdot e^{-\frac{E}{k_B \cdot T}} \left( 1 + \frac{s \cdot n_0}{N \cdot \beta} \int_{T_0}^T e^{-\frac{E}{k_B \cdot \tau}} d\tau \right)^{-2}. \quad (2.7)$$

The luminescence is proportional to  $n_0^2$  for which it is called second order kinetics. The peak here is more symmetric and spreads wider. This is a result of detrapped electrons being retrapped. The emission of luminescence is delayed and also more distributed considering the temperature.

### General Order Kinetics

A general model has been proposed where the time rate of change of the population density is given by

$$\frac{dn}{dt} = -n^b \cdot s' \cdot e^{-\frac{E}{k_B \cdot T}} \quad (2.8)$$

b....order of kinetics;  $b \neq 1$

$s'$ ...pre-exponential factor;  $[cm^3(b-1)s^{-1}]$

and the luminescence intensity can be obtained by (Basun et al., 2003) [11]

$$I(T) = -\frac{dn}{dt} = n^b \cdot s' \cdot e^{-\frac{E}{k_B \cdot T}} \left( 1 + (b-1) \cdot n_0^{b-1} \frac{s'}{\beta} \int_{T_0}^T e^{-\frac{E}{k_B \cdot \tau}} d\tau \right)^{-\frac{b}{b-1}}. \quad (2.9)$$

Calculation of the parameters in equation (2.9) might be difficult as  $s'$  depends on  $b$  for example. A novel method for determining the parameters however is discussed in Rawat et al. (2009) [12].

## 2.5 Effects Affecting Thermoluminescence Dating

### 2.5.1 Anomalous Fading

Anomalous fading describes the effect when a sample shows a time-dependent instability of its glow-curve. These instabilities relate to the amount of dose the sample receives (Li and Li, 2008) [13] but they are hardly temperature related and probably occur due to quantum-mechanical tunnelling (Aitken, 1985) [2]. Electrons can tunnel to recombination centers with some probability without being supplied with additional energy. Other more recently discussed possibilities are radiation- and temperature-induced ionic processes (Jaek et al., 2007) [14].

In order to detect the effect of anomalous fading some of the samples are, additionally to their natural dose, irradiated with a well-known dose. Then a part of the samples is measured [see Fig. 2.5 (a)] . The other part is stored for 15 hours at  $-18^{\circ}\text{C}$  [see Fig. 2.5 (b)].

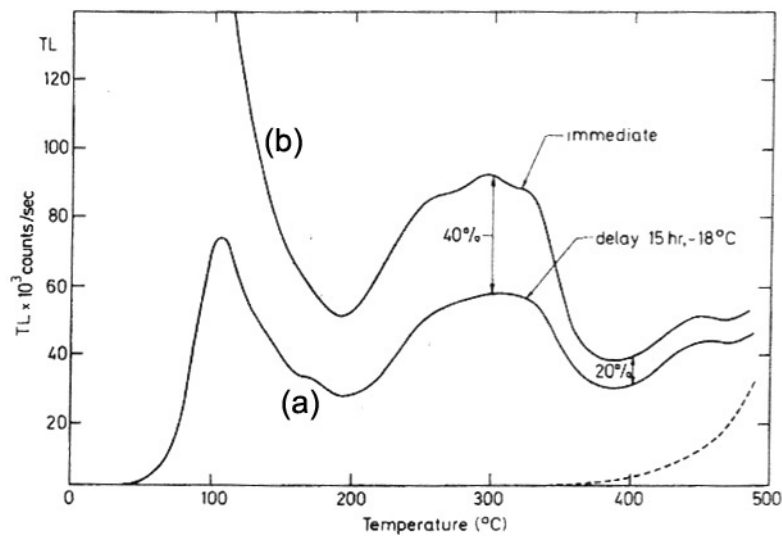


Figure 2.5: Anomalous fading of a brick; (a) glow-curve of the immediately irradiated and measured sample; (b) glow-curve of the sample which was stored for 15 hours at  $-18^{\circ}\text{C}$  after irradiation and then measured; (Aitken, 1985) [2]

Because of anomalous fading the underestimation of an age of 10,000 years for thermoluminescence is averaged to 5 % by Zink (2008) [15]. A numerical model for describing the effect of fading in feldspars was developed by Larsen et al. (2009) [16].

### 2.5.2 Bleaching

The thermoluminescence signal of a sample can be reduced when it is exposed to light. Electrons can be excited optically and leave traps. Hence, they are able to reach empty recombination centers and thereby emit light. Therefore, it is necessary to deal with the sample during preparation and measurement under red light.

In Fig. 2.6 this effect can be seen on the basis of a limestone sample. The bleaching took place in a solar simulator and (b) shows the glow-curve after 4 minutes of bleaching and (c) after 80 hours of bleaching.

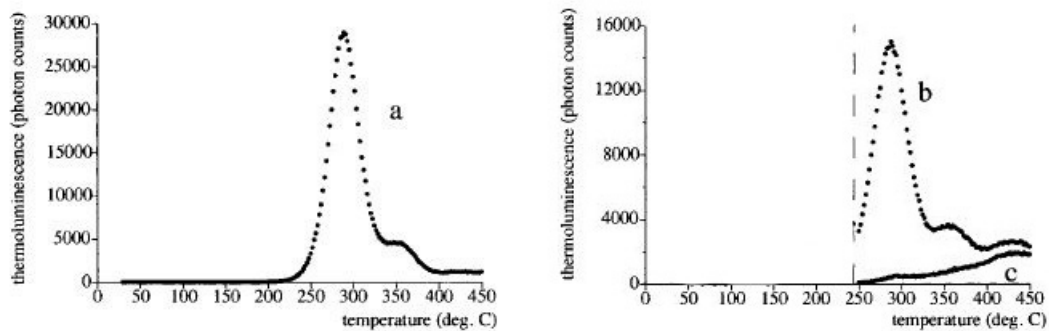


Figure 2.6: Bleaching of a limestone sample; (a) natural glow-curve unbleached; (b) after bleaching for 4 min; (c) after bleaching for 80 h; adapted from Bruce et al. (1999) [4]

### 2.5.3 Spurious Thermoluminescence

Spurious thermoluminescence describes luminescence adding to the thermoluminescence signal which is not induced by radiation.

Chemiluminescence for example makes a contribution. Chemical reactions can occur at room temperature or at increased temperature during the measurement. Other possibilities are the appearances of bioluminescence and triboluminescence. In order to reduce “spurious thermoluminescence” the metering chamber is filled with pure nitrogen.

Furthermore, fine-grains are more sensitive to spurious thermoluminescence than larger ones.

#### **2.5.4 Thermal Instability**

Due to irradiation during the measuring process thermal instable traps can be built or filled with electrons. As these traps would contribute to a larger thermoluminescence signal, it is necessary to empty them first. In the process, samples are pre-heated at 190 °C for a minute in order to dissipate unstable traps.

Deeper traps, which are important for the dating process, are hardly influenced.

#### **2.5.5 Thermal Quenching**

This effect describes the decrease of thermoluminescence efficiency while the temperature increases. It can be explained by the fact that the probability of an excited electron returning to the ground state by emitting light is smaller than the probability of inducing a phonon by doing so.

This process is sensitive to temperature and can be neglected for low temperatures.

### **2.6 Plateau Test**

The plateau test indicates the equivalency of two glow-curves that only vary in their proportionality. This proportionality can usually be observed only for a certain temperature interval. The ratio between a natural glow-curve and an additionally irradiated one is determined. Fig. 2.7 shows such glow-curves: natural glow-curve (turquoise), differently irradiated glow-curves (red, black, blue, green) and the ratios (lilac, purple, brown, violet).

The reason for not being proportional throughout the whole temperature area might be that the sensitivity of the material changes because of the high dose rates which are used while irradiating in the laboratory in comparison to the much lower natural dose rates. Traps, however, that lie deep enough and therefore need an accordingly high temperature to be emptied are responsible for the proportionality. Another possibility why the ratio is not constant could be a consequence of anomalous fading as discussed in section 2.5.1 where the luminescence is not radiation-induced.

The interval where the ratios are constant is called plateau and is used as analysis area. An interval has to be chosen in which fluctuations are not too large. If there is no plateau to be observed, the age of the sample cannot be determined. Although, it is possible that due to the heating contacts during the heating process the glow-curves are shifted slightly and the maxima are not found at exactly the same temperature. In that case, the constancy of the plateau would be affected and a correlation function implemented in the dating software (Gratzl, 1989) [17]



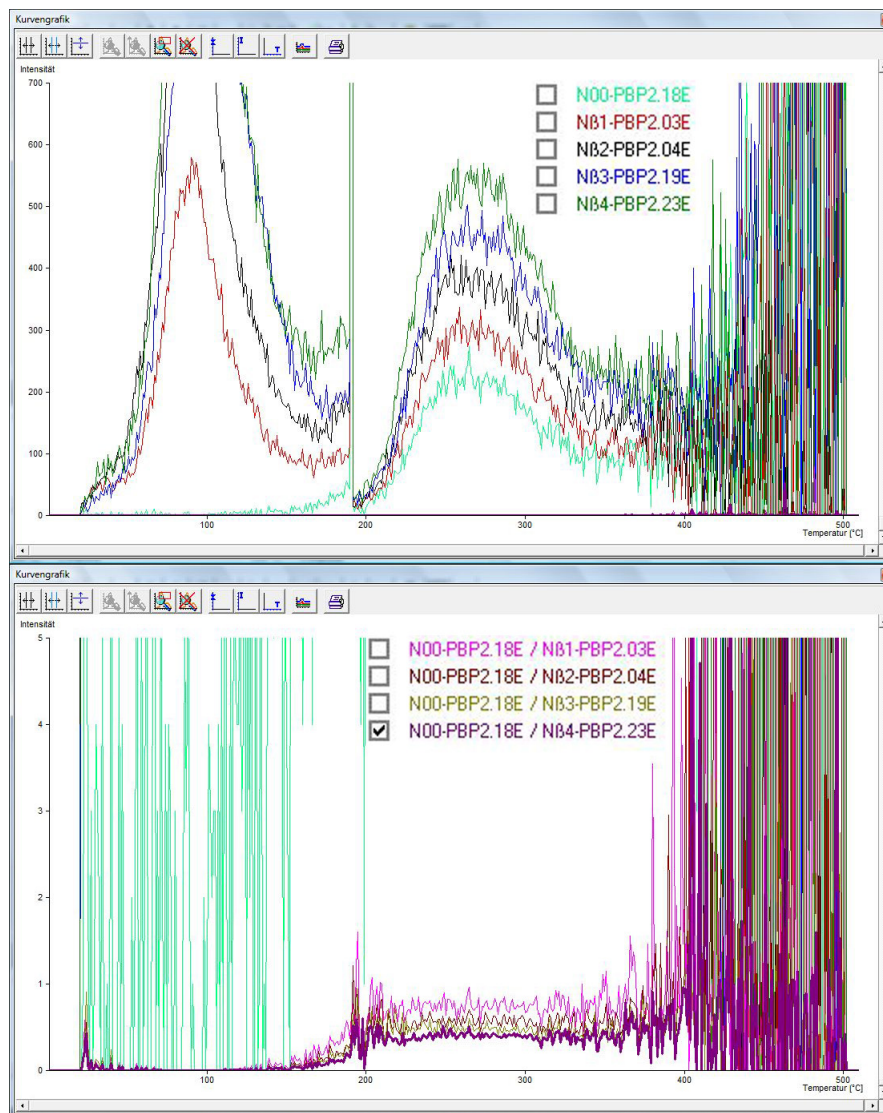


Figure 2.7: Plateau test; (a) natural and artificial irradiated glow-curves; (b) ratios of the glow-curves;

could be applied. The average curve of all glow-curves is calculated and the individual curves are shifted according to this average curve.

The correlation function is given by

$$k(x) = \int_a^b f(x')g(x' - x)dx' \quad (2.10)$$

and the x-coordinate ( $x_m$ ) of the maximum of  $k(x)$  is calculated. Now the curves are shifted, either by  $f$  for  $x_m$  or by  $g$  for  $-x_m$  until they are in agreement. The interval  $[a, b]$  is determined by observing the glow-curves and the plateau interval.

## 2.7 Determination of the Paleodose Using the Additive Method

The paleodose can be determined by comparison of the natural thermoluminescence and the thermoluminescence, which comes from samples that were irradiated with a well-known dose. The additive method is discussed in detail by Aitken (1985) [2]

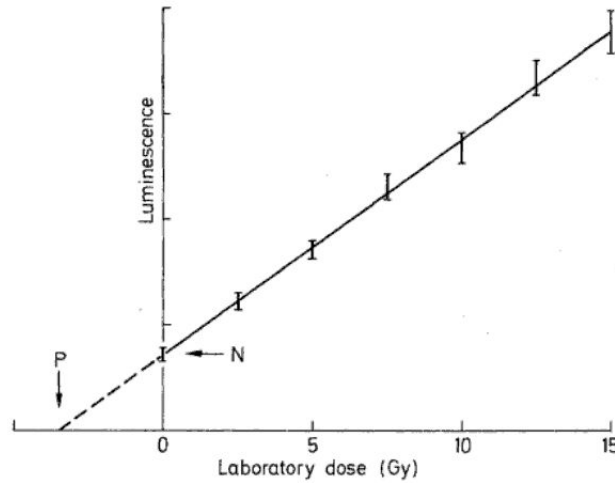


Figure 2.8: The additive method (Aitken, 1998) [5]

A number of samples is prepared (see section 3.2) and the first measurements determine the natural thermoluminescence of a part of the samples. The rest is irradiated with different but well-known doses and also measured. Fig. 2.8 shows the different measuring points, where  $N$  is the obtained natural thermoluminescence signal and the others are the ones obtained by irradiating the samples with

a  $\beta$ -source. The luminescence signal increases with the dose and linear response between these two is assumed. The straight line is extrapolated until it intersects with the x-*abscissa*. This extrapolation is necessary as the connection between the luminescence signal and the dose can only be determined in the area above the natural luminescence. Hence the  $\beta$ -equivalent dose (Q) is obtained which in this case is the same as the paleodose (P).

The paleodose, however, is not necessarily equivalent to the equivalent dose but usually greater. This is due to the supra-linearity of the luminescence signal. As can be seen in Fig. 2.9, where samples have been irradiated and measured after the first glow, the increase of the thermoluminescence with dose is not linear but supra-linear at low doses. I is the intercept which corrects the supra-linearity and has to be added to the  $\beta$ -equivalent dose in order to receive the paleodose (Fig. 2.10). A condition for doing so is that the  $\beta$ - and second-glow-regression lines are parallel. This supra-linearity effect (Fig. 2.11) occurs at low doses and does not occur while using  $\alpha$ -particles for irradiation. It can be explained by the interaction between the traps (Aitken, 1985) [2]. Another effect (Fig. 2.11) appears at high doses, the sub-linearity. It occurs due to saturation of the electron traps at sufficiently large doses.

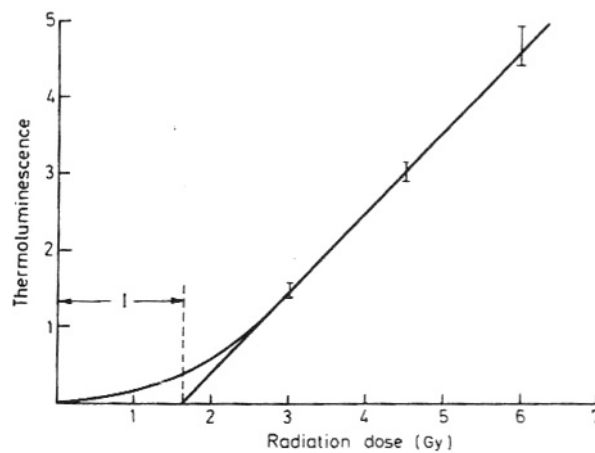


Figure 2.9: Supra-linearity correction in second-glows (Aitken, 1985) [2]

## 2.8 Fine-Grain Dating

This method is discussed by Aitken (1985) [2].

The grains used for this technique have to be completely penetrated by the internal  $\alpha$ -,  $\beta$ - and  $\gamma$ -radiation as well as the external  $\gamma$ -radiation. In order to assure this, the obtained grains have to be small enough (approx. 1-8  $\mu\text{m}$  in diameter). The

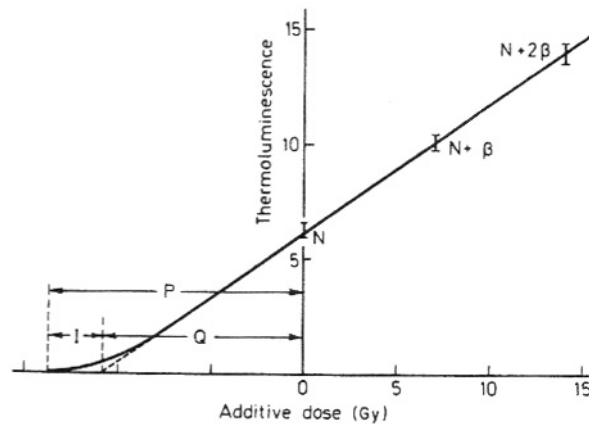


Figure 2.10: Determination of the paleodose considering the intercept (Aitken, 1985) [2]

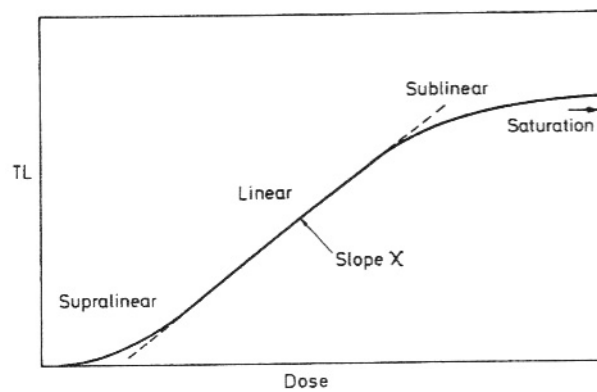


Figure 2.11: Supra- and sub-linearity (Aitken, 1985) [2]

first 2 mm of the surface of the sample have to be removed so as to neglect the external  $\alpha$ - and  $\beta$ -radiation. Furthermore, the  $\alpha$ -efficiency (see section 2.9.1) has to be considered.

## 2.9 Age Calculation

Thermoluminescence for a good portion of samples comes from the radiation of radionuclides such as uranium, thorium (and their decay products) and potassium. Additionally, the decay of rubidium and cosmic radiation have to be considered although they only add a small percentage to total radiation.

Thermoluminescence is proportional to the amount of absorbed energy.  $\beta$ -radiation, which has a share in the annual dose rate, is mostly emitted by radioisotopes within the sample. Only at the surface the  $\beta$ -radiation of the surrounding soil also has to be taken into account.  $\gamma$ -radiation contributing to the annual dose rate on the other hand is nearly completely emitted by materials surrounding the sample.

Formulas needed for the age calculation are originally from Aitken (1985) [2] and have been adapted by Gratzl (1989) [17] and Bergmann (2005) [18]. They are included in the dating software described in section 3.3.3.

For fine-grain dating the age of the sample is given by

$$Age[a] = \frac{P}{\dot{D}} = \frac{Q_{\beta} + I}{\dot{D}'_{\alpha} + \dot{D}_{\beta} + \dot{D}_{\gamma} + \dot{D}_c} \quad (2.11)$$

$P$ .....paleodose [Gy/a]

$\dot{D}$ .....annual dose rate [Gy/a]

$Q_{\beta}$ ..... $\beta$ -equivalent dose [Gy]

$Q_{\alpha}$ ..... $\alpha$ -equivalent dose [Gy]

$a$ ..... $\alpha$ -efficiency:  $a = \frac{Q_{\beta}}{Q_{\alpha}}$

$I$ .....intercept [Gy]

$\dot{D}'_{\alpha}$ .....effective  $\alpha$ -dose rate [Gy/a]:  $\dot{D}'_{\alpha} = a \cdot \dot{D}_{\alpha}$

$\dot{D}_{\alpha,\beta,\gamma}$ ... $\alpha$ -,  $\beta$ -,  $\gamma$ -dose rate [Gy/a]

$\dot{D}_c$ .....cosmic dose rate [Gy/a]

For inclusion dating (grains with approx. 100  $\mu\text{m}$   $\varnothing$ ) the age of the sample is given by

$$Age[a] = \frac{Q_\beta + I}{b \cdot \dot{D}_\beta + \dot{D}_\gamma + \dot{D}_c} \quad (2.12)$$

$b \dots \beta$ -attenuation: 0.9 for inclusion dating

It is assumed that the laboratory studies are accomplished with a dry sample. As the sample might have taken up water during its storage in the ground some corrections to the dose rates have to be applied by means of equations (2.20) and (2.21).

### 2.9.1 $\alpha$ -Efficiency

A sample irradiated with a certain dose rate by an  $\alpha$ -source provides a far less thermoluminescence intensity than a sample irradiated with the same dose rate by a  $\beta$ - or  $\gamma$ -source. This effect occurs due to saturation which takes place as a result of the high ionization density that an  $\alpha$ -particle produces along its track.

Consequently the so-called  $\alpha$ -efficiency ( $a$ ) is established as

$$a = \frac{TL_{N+\alpha} - TL_N}{TL_{N+\beta} - TL_N} \frac{\dot{D}_\beta}{\dot{D}_\alpha} \quad (2.13)$$

$TL_{N+\alpha} \dots$  TL intensity of a natural sample irradiated by an  $\alpha$ -source

$TL_{N+\beta} \dots$  TL intensity of a natural sample irradiated by a  $\beta$ -source

$TL_N \dots$  TL intensity of a natural sample

and can be calculated by comparing the equivalent doses  $Q_\alpha$  and  $Q_\beta$  of several irradiated samples

$$a = \frac{Q_\beta}{Q_\alpha} \quad (2.14)$$

whereas its standard deviation is given by

$$da = \frac{Q_\alpha \delta Q_\beta - Q_\beta \delta Q_\alpha}{Q_\alpha^2}. \quad (2.15)$$

In consideration of the definition of the  $\alpha$ -efficiency, the  $\alpha$ -dose rate now delivers the same thermoluminescence intensity as the  $\beta$ -dose rate with  $\dot{D}_\beta = a \cdot \dot{D}_\alpha$ , and the total annual dose rate ( $\dot{D}$ ) consists of

$$\dot{D} = a \cdot \dot{D}_\alpha + \dot{D}_\beta + \dot{D}_\gamma + \dot{D}_c. \quad (2.16)$$

### 2.9.2 $\alpha$ -Dose Rate

The  $\alpha$ -particles emitted from the sample are counted by an  $\alpha$ -counter and it can be distinguished between  $\alpha$ -particles, which accrue from the thorium decay series and others from the uranium decay series. The discrimination is achieved through the so-called “pair counting” method which is realized via a coincidence circuit. “Slow  $\alpha$ -pairs” in the Th-decay series  $^{220}\text{Rn} \rightarrow ^{216}\text{Po}$  ( $T_{\frac{1}{2}} = 0.15 \text{ s}$ ) are distinguished from “fast  $\alpha$ -pairs” in the U-decay series  $^{219}\text{Rn} \rightarrow ^{215}\text{Po}$  ( $T_{\frac{1}{2}} = 0.0018 \text{ s}$ ) as the coincidence window of the used  $\alpha$ -counter is opened from 0.02 to 0.4 s after every decay and only the “slow pairs” are detected (Hossain et al., 2002) [19].

The amount of  $\alpha$ -particles of the Th-decay series ( $\alpha_{Th}$ ) per ks can therefore be calculated by (Aitken, 1985) [2]

$$\alpha_{Th} = 21 \cdot \left( d - \frac{0.38 \cdot \alpha^2}{1000} \right), \quad (2.17)$$

$d$ ...amount of coincidence pairs/ks

$\alpha$ ...amount of counted  $\alpha$ -particles/ks

whereas the amount of  $\alpha$ -particles of the U-decay series ( $\alpha_U$ ) per ks can be obtained by

$$\alpha_U = \alpha - \alpha_{Th}. \quad (2.18)$$

If the sample contains only members of the thorium series, the  $\alpha$ -dose rate will be obtained by  $\dot{D}_\alpha = 1480 \cdot \alpha$  and for samples which include only the uranium series the  $\alpha$ -dose rate is defined by  $\dot{D}_\alpha = 1640 \cdot \alpha$  (Aitken, 1985) [2]. These dose rates have still to be modified by special values for the thorium- and uranium-dose and hence the effective  $\alpha$ -dose rate is given by

$$\dot{D}'_\alpha [mGy/a] = a \cdot \frac{1.2728 \cdot \alpha_{Th} + 1.2792 \cdot \alpha_U}{1 + 1.5 \cdot W \cdot F} \quad (2.19)$$

additionally taking into account the effect of moisture as described in following equations (2.20) and (2.21):

$$W = \frac{S - T}{T} \quad (2.20)$$

$$F = \frac{A}{S} \quad (2.21)$$

$W$ ...saturation weight increase  
 $F$ ....wetness fraction  
 $A$ ....weight of wet sample  
 $S$ ....saturation fraction  
 $T$ ....weight of dry sample

If the thorium/uranium-ratio is not determined but the same activity for both decay series is assumed, the average value of the coefficients in the numerator in equation (2.19) will be used and the effective  $\alpha$ -dose rate results in

$$\dot{D}'_{\alpha} [mGy/a] = a \cdot \frac{1.2760 \cdot \alpha}{1 + 1.5 \cdot W \cdot F}. \quad (2.22)$$

### 2.9.3 $\beta$ -Dose Rate

The  $\beta$ -dose rate contains all the decays of thorium, uranium, potassium and rubidium:

$$\dot{D}_{\beta} [mGy/a] = \dot{D}_{\beta,Th,U} + \dot{D}_{\beta,K,Rb} \quad (2.23)$$

The  $\beta$ -dose rate originating from the thorium- and uranium-decay series is given by (Aitken, 1985) [2]

$$\dot{D}_{\beta,Th,U} [mGy/a] = b \cdot \frac{0.057 \cdot \alpha_{Th} + 0.087 \cdot \alpha_U}{1 + 1.25 \cdot W \cdot F} \quad (2.24)$$

in which  $b$  again is the attenuation of the  $\beta$ -radiation and considers the grain size ( $b = 1$  for fine grains).



If the thorium/uranium-ratio is not determined but the same activity for both decay series is assumed, the average value of the coefficients in the numerator in equation (2.24) will be used and the  $\beta$ -dose rate results in

$$\dot{D}_{\beta,Th,U} [mGy/a] = b \cdot \frac{0.072 \cdot \alpha}{1 + 1.25 \cdot W \cdot F}. \quad (2.25)$$

The  $\beta$ -dose rate caused by  $^{40}\text{K}$  in a sample with 1 %  $\text{K}_2\text{O}$  is 0.689 mGy/a. If the rubidium concentration in the sample is not determined, a potassium/rubidium-ratio of usually 200:1 will be assumed. This means that there are 50 ppm  $\text{Rb}_2\text{O}$  per 1 %  $\text{K}_2\text{O}$  and the  $\beta$ -dose rate amounts to 0.019 mGy/a. The total resulting  $\beta$ -dose rate per 1 %  $\text{K}_2\text{O}$  concentration in the sample adds up to 0.708 mGy/a.

$$\dot{D}_{\beta,K,Rb} [mGy/a] = b \cdot \frac{0.708 \cdot m}{1 + 1.25 \cdot W \cdot F} \quad (2.26)$$

$m$ ...weight of  $\text{K}_2\text{O}$  in the sample in %

#### 2.9.4 $\gamma$ -Dose Rate

The  $\gamma$ -dose rate can be separated into an internal contribution, caused by radioactive isotopes within the sample, and an external contribution depending on the surrounding soil.

$$\dot{D}_{\gamma} [mGy/a] = \dot{D}_{\gamma int} + \dot{D}_{\gamma ext} \quad (2.27)$$

The internal  $\gamma$ -dose rate, however, is made up by a part considering the decay of thorium and uranium and another part considering the decay of potassium.

$$\dot{D}_{\gamma int} [mGy/a] = \dot{D}_{\gamma int,Th,U} + \dot{D}_{\gamma int,K} \quad (2.28)$$

The internal  $\gamma$ -dose rate induced by thorium and uranium is given by (Aitken, 1985) [2]

$$\dot{D}_{\gamma int,Th,U} [mGy/a] = \frac{0.103 \cdot \alpha_{Th} + 0.068 \cdot \alpha_U}{1 + 1.14 \cdot W \cdot F}. \quad (2.29)$$

If the thorium/uranium-ratio is not determined but the same activity for both decay series is assumed, the average value of the coefficients in the numerator in equation (2.29) will be used and the internal  $\gamma$ -dose rate results in

$$\dot{D}_{\gamma_{int,Th,U}} [mGy/a] = \frac{0.085 \cdot \alpha}{1 + 1.14 \cdot W \cdot F}. \quad (2.30)$$

On the other hand the internal  $\gamma$ -dose rate induced by potassium is given by

$$\dot{D}_{\gamma_{int,K}} [mGy/a] = \frac{0.241 \cdot m}{1 + 1.14 \cdot W \cdot F}. \quad (2.31)$$

These dose rates are only applicable for infinitely expanded samples, therefore dose rates of finitely expanded samples have to be corrected by multiplying them with the self-attenuation factor  $p/100$ .  $p$  then shows the percentage of the  $\gamma$ -dose rate within the sample caused by the sample itself corresponding to the dose rate within a sample with the same radioactivity but infinite expansion.

In accordance with the superposition principle the dose rate within the sample induced by external radiation is given by  $(1 - \frac{p}{100}) \cdot \dot{D}_{\gamma_{ext}}$ .  $\dot{D}_{\gamma_{ext}}$  comes from the “infinite” soil surrounding the sample.

The self-dose percentage is estimated and given by (Aitken, 1985) [2]

$$p = 100 \cdot (1 - \exp^{-0.06 - 0.07 \cdot d}) \quad (2.32)$$

for a parallely sided sample where  $d$  refers to the sample thickness and

$$p = 2 \cdot d \quad (2.33)$$

for spheric samples with diameter  $d$ .

Thus the adjusted  $\gamma$ -dose rate results in

$$\begin{aligned} \dot{D}_{\gamma} &= \frac{p}{100} \cdot \dot{D}_{\gamma_{int}} + \left(1 - \frac{p}{100}\right) \cdot \dot{D}_{\gamma_{ext}} = \\ &= \frac{p}{100} \cdot (\dot{D}_{\gamma_{int,Th,U}} + \dot{D}_{\gamma_{int,K}}) + \left(1 - \frac{p}{100}\right) \cdot \dot{D}_{\gamma_{ext}}. \end{aligned} \quad (2.34)$$

For the measurement of the external  $\gamma$ -dose rate two possibilities are available: On the one hand, a scintillation counter can be used. This method is rather uncomplicated and delivers fast results but one has to be aware that moisture fluctuations, due to different seasons, affect the result.

The other way of measuring is to use thermoluminescence dosimeters which are based upon the same principle as luminescence dating. These dosimeters are buried in the soil at the excavation site. They are covered by special cases so that the  $\beta$ -radiation is shielded. The resulting  $\gamma$ -dose rate has to be multiplied with a correction factor (approx. 1.1) because the  $\gamma$ -radiation is also partly shielded. With this method the fluctuations of moisture are considerably less because the measurement lasts for a few weeks or months and changing environmental influences are included.

Whatever method is chosen the cosmic dose rate is part of the measured  $\gamma$ -dose rate and has to be subtracted. Additionally, the moisture during measurement and storage of the sample has to be taken into account again and the external  $\gamma$ -dose rate is therefore obtained by:

$$\dot{D}_{\gamma ext} = \dot{D}_{\gamma TLD} \cdot \frac{1 + 1.14 \cdot W_S \cdot F_S}{1 + 1.14 \cdot W_S \cdot F} - \dot{D}_c \quad (2.35)$$

$F_S$ ....wetness of soil

$W_S$ ...saturation weight increase of soil

### 2.9.5 Cosmic Dose Rate

Cosmic radiation impinges Earth from space and can be divided in primary and secondary radiation. Primary radiation mostly consists of protons and a few nuclei with higher atomic mass. These particles are affected by the geomagnetic field and by the atmosphere (Prescott and Stephan, 1982) [6]. In the atmosphere they interact with air molecules and produce secondary radiation, which is mainly made up of electrons, photons, muons, neutrons, protons and other hadrons as well as by a neutrino flux. As these progenies are not completely absorbed, they can reach the Earth surface and cause an additional luminescence signal. Therefore, the contribution of the cosmic dose rate depends on height but is usually small compared to the terrestrial dose rate. For many sediments it is less than 5 % (Liritzis, 2000) [20] and can be found in special radiation maps or calculated, as shown in equation 3.9.

## 2.10 Error Estimation

All kinds of errors that could possibly occur during the measurement have to be taken into account and will be displayed as a percentage error of the calculated age. This procedure is explained by Aitken (1985) [2]. Formulas which were used have been adapted by Gratzl (1989) [17] and are included in the dating software described in section 3.3.3.

On the one hand there are statistical (random) errors which describe the deviation from the measured results. They do not correlate with errors of another sample of the same object and can be reduced by increasing the amount of individual measurements.

Systematic errors on the other hand are errors which are reproduced each time when a measurement is repeated under the same conditions and deliver the same result for each measured sample of any object (e.g. an imprecision in the calibration of the radiation source). These errors cannot be reduced by increasing the amount of individual measurements.

It will be assumed that the errors can be described by a Gaussian distribution function with the standard deviation  $\sigma$ . Therefore, the true date lies within this limit with a probability of  $\pm 68\%$ . The total error is derived from the square root of the sum of the squares of the individual errors.

$$\sigma_{tot} = \sqrt{\sigma_{ran}^2 + \sigma_{sys}^2} \quad (2.36)$$

$\sigma_{tot}$ ....total error  
 $\sigma_{ran}$ ....statistical (random) error  
 $\sigma_{sys}$ ....systematic error

The following abbreviations are used for the contribution of each individual dose to the annual dose.

$$\begin{aligned} f_{\alpha} &= \frac{\dot{D}'_{\alpha}}{\dot{D}}, f_{\beta} = \frac{\dot{D}_{\beta}}{\dot{D}}, f_{\gamma} = \frac{\dot{D}_{\gamma}}{\dot{D}}, \\ f_{\beta,Th,U} &= \frac{\dot{D}_{\beta,Th,U}}{\dot{D}}, f_{\beta,K,Rb} = \frac{\dot{D}_{\beta,K,Rb}}{\dot{D}}, \\ f_{\gamma,int} &= \frac{\dot{D}_{\gamma,int}}{\dot{D}}, f_{\gamma,int,Th,U} = \frac{\dot{D}_{\gamma,int,Th,U}}{\dot{D}}, f_{\gamma,int,K} = \frac{\dot{D}_{\gamma,int,K}}{\dot{D}}, f_{\gamma,ext} = \frac{\dot{D}_{\gamma,ext}}{\dot{D}} \end{aligned} \quad (2.37)$$

### 2.10.1 Statistical (Random) Errors

The total random error is given by

$$\sigma_{ran}^2 = \sum_{i=1}^3 \sigma_i^2. \quad (2.38)$$

$\sigma_1$ ...error in thermoluminescence measurement

$\sigma_2$ ...error in assessing the annual dose rate

$\sigma_3$ ...error caused by stony surroundings

### Thermoluminescence Measurement

$Q_\alpha$ ,  $Q_\beta$  and  $I$  are assessed during the thermoluminescence measurement and their uncertainties are given by  $\delta Q_\alpha$ ,  $\delta Q_\beta$  and  $\delta I$ . These values are the standard deviations of the measured valuables and are not correlated. The error calculation leads to (Aitken, 1985) [2]

$$\sigma_1^2 = \left[ 100 \cdot \left( 1 - \frac{Q_\beta + I}{Q_\beta} \cdot f_\alpha \right) \cdot \frac{\delta Q}{Q + I} \right]^2 + \left( \frac{100 \cdot \delta I}{Q + I} \right)^2 + \left( 100 \cdot f_\alpha \cdot \frac{\delta Q_\alpha}{Q_\alpha} \right)^2 \quad (2.39)$$

### Annual Dose Rate

The uncertainty in  $\alpha$ -counting rate and the errors in determination of the potassium concentration and the  $\gamma$ -thermoluminescence dosimetry are not correlated and hence the error is given by (Gratzl, 1989) [17]

$$\sigma_2^2 = 25 \cdot \left[ (f_\alpha + f_{\beta,Th,U} + f_{\gamma int,Th,U})^2 + (f_{\beta,K,Rb} + f_{\gamma int,K})^2 + f_{\gamma ext}^2 \right]. \quad (2.40)$$

Otherwise  $f_\alpha$ ,  $f_{\beta,Th,U}$  and  $f_{\gamma int,Th,U}$  can be simply summed-up because their dose rates are determined by the same procedure ( $\alpha$ -counting rate). Thus, they are correlated.  $f_{\beta,K}$  and  $f_{\gamma int,K}$  can analogously be dealt with. Moreover, it is assumed that the errors in the individual dose rates are about  $\pm 5 \%$ .

## Stony Surroundings

There is another uncertainty if there are stones or rocks surrounding the sample in the soil, as they can be responsible for scattering or shielding. The error estimation leads to (Aitken, 1985) [2]

$$\sigma_3^2 = 100 \cdot r \cdot f_\gamma \cdot \left( \frac{\dot{D}_1 - \dot{D}_2}{\dot{D}_\gamma} \right) \quad (2.41)$$

$\dot{D}_1$ ... $\gamma$ -dose rate of surrounding soil

$\dot{D}_2$ ... $\gamma$ -dose rate of stones

r.....actual weight component of stones in surroundings of sample

### 2.10.2 Systematic Errors

The total systematic error is given by

$$\sigma_{sys}^2 = \sum_{i=4}^6 \sigma_i^2. \quad (2.42)$$

$\sigma_4$ ...error due to calibration

$\sigma_5$ ...error in thorium/uranium ratio

$\sigma_6$ ...error due to wetness

## Calibration

Thermoluminescence dating is a procedure which gives the absolute date of a sample. Because of that it is important to consider the errors arising from the calibration of the  $\alpha$ -counter, the used  $\alpha$ -, $\beta$ -radiation sources and the  $K_2O$ -standard utilized for the determination of potassium. The error is given by (Gratzl, 1989) [17]

$$\sigma_4^2 = 25 \cdot [f_\alpha^2 + (1 - f_\alpha)^2 + (f_\alpha + f_{\beta,Th,U} + f_{\gamma int,Th,U})^2 + (f_{\beta,K,Rb} + f_{\gamma int,K})^2 + f_{\gamma ext}^2] \quad (2.43)$$

## Thorium/Uranium-Ratio

The  $\beta$ -dose rate is derived from the  $\alpha$ -counting rate and therefore it is assumed that the thorium and uranium activity in the sample are the same. But even if one or the other dominates, the maximum error in the  $\beta$ -dose rate is  $\pm 20$  % according to equations (2.24) and (2.25). The maximum error in the internal  $\gamma$ -dose rate is as well  $\pm 20$  % according to equations (2.29) and (2.30). Thus, the error can be described as

$$\sigma_5 = 14 \cdot |f_{\beta,Th,U} - f_{\gamma_{int},Th,U}| \quad (2.44)$$

## Wetness

As there are uncertainties ( $\delta F$ ) about how much water the sample has absorbed during its storage another error has to be taken into account. Past site rainfall and drainage have to be considered, hence the error in the age is given by (Gratzl, 1989) [17]

$$\sigma_6 = 100 \cdot [(1.5 \cdot f_{\alpha} + 1.25 \cdot f_{\beta} + 1.14 \cdot f_{\gamma_{int}}) \cdot W + 1.14 \cdot f_{\gamma_{ext}} \cdot W_S] \cdot \delta F \quad (2.45)$$

For commonly analyzed samples with  $W = 0.2$  and  $W_S = 0.3$  and  $\delta F$ ,  $\sigma_6$  is approximately 5.9 % for the fine-grain method and 5.8 % for the inclusion method.

## 3 Experiment Preparation and Execution

### 3.1 Parameters of Age Determination

This section comprises procedures that are necessary for the determination of additional parameters.

#### 3.1.1 Thorium/Uranium-Ratio

For the determination of  $\alpha$ -counting a Daybreak 582  $\alpha$ -counter was used whereby the emitted  $\alpha$ -particles can be separated for the thorium and uranium series. The principle of its functionality is shown in Fig. 3.1.

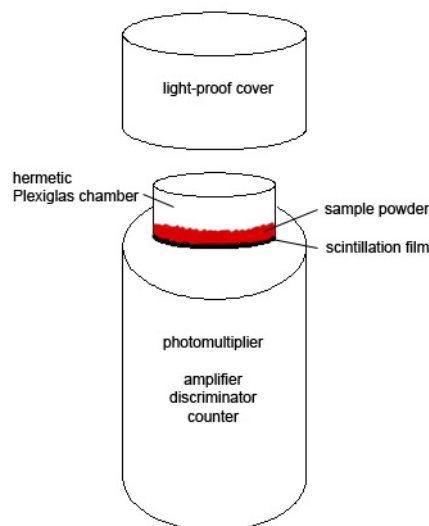


Figure 3.1:  $\alpha$ -counting system

The  $\alpha$ -counter consists of a photomultiplier and a air-tight Plexiglas chamber enclosed in a light-proof box. A scintillation film with a diameter of 42 mm is placed on the bottom of the chamber. On this film the sample powder (approx. 0.2 g) is spread with a coating thickness of approximately 0.1 mm. The screen has to be completely covered and is placed within the chamber which is then hermetically sealed. The zinc-sulfide coating of the scintillation film is excited by  $\alpha$ -radiation and emits flashes of light. These flashes reach the photocathode of the photomultiplier and produce photoelectrons which are onward multiplied. By means of the discriminator the  $\beta$ - and  $\gamma$ -radiation can be neglected. The total counts per ks are displayed and the pair-counts are obtained as explained in section



2.9.2. The activities of the thorium-series and the uranium-series are given by (Aitken, 1985) [2]

$$c_{Th} = \frac{1}{0.0048}d \quad (3.1)$$

$$c_U = \frac{1}{0.132}(\alpha - 0.123c_{Th}). \quad (3.2)$$

$d$ ...amount of coincidence pairs/ks

$\alpha$ ...amount of counted  $\alpha$ -particles/ks

A weight component of 1 ppm  $^{232}\text{Th}$  causes an activity of 4.08 Bq/kg while 1 ppm of natural uranium causes an activity of 13 Bq/kg (Aitken, 1985) [2].

Hence the proportions of weight for thorium and uranium in ppm are:

$$ppm_{Th} = \frac{c_{Th}}{4.08} \quad (3.3)$$

$$ppm_U = \frac{c_U}{13} \quad (3.4)$$

Before measuring a sample the background rate has to be determined. For that purpose a measurement is made by using only the scintillation film placed in the Plexiglas chamber without the sample powder. Measurement goes on for a period of four days and afterwards the process is repeated with the spreaded sample powder on the film (approx. 5-7 days). The analysis is made with the program module described in section 3.3.3 by filling in the start and end date of the measurements and the obtained counting rates.

### 3.1.2 Wetness Corrections

If the sample has accumulated much water during its burial in the ground, a part mainly of the  $\alpha$ -radiation is absorbed by the water molecules and therefore the results have to be modified. These parameters are often estimated because it is not always possible to carry out all necessary measurements at the excavation site.

First of all the weight of the found wet sample has to be determined in order to obtain the weight proportion of water in the sample. This value could be influenced by transport and storage. A little sliver of the sample is separated

and weighed immediately. After that it is dried in the oven during four days and weighed again to obtain the dry weight. In a final step the fragment is stored in distilled water for four days and by weighing it the last needed value, the saturation weight, is determined. Hence the saturation fraction and saturation weight increase can be calculated with equations (2.20) and (2.21).

### **3.1.3 Determination of Potassium Concentration by Neutron Activation Analysis**

This technique is based on the principle that a sample is irradiated by thermal neutrons and the produced radio nuclides emit characteristic  $\gamma$ -rays which are measured. This procedure is performed in a nuclear reactor. If the elemental concentrations are not known, the sample is irradiated along with a standard of known elemental concentrations. The intensities of the characteristic radiations of the sample and the standard are compared and the potassium concentration of the sample can be determined after an appropriate radioactive decay and measuring the gamma energy spectrum. Two standards have been used with 2.64 % and 1.95 % potassium.

#### **Sample Preparation**

1. Powder of the sample (approx. 200 mg) has to be obtained either by drilling a little hole or by splitting off small fragments of the sample with hammer and chisel. It has to be kept in mind that the chemical composition of the powder can be affected when it is excessively breathed upon.
2. Then the powder is put into a mortar and further pulverized before being stored in a clean little glass container.
3. In order to dehumidify the sample powder and therefore to avoid the influence of the humidity on the measurement results the container is put into an oven for 24 hours at 110 °C.
4. Afterwards the powder is weighed and filled into polyethylene casings, which should be contacted only with tweezers in order to avoid adulteration of the results. It is absolutely vital that the casings are sealed properly as otherwise radioactive substances can leak after irradiation. The same is done with a standard material and the casings are labelled.
5. These polyethylene casings are placed into a larger irradiation capsule which is given to a staff member of the reactor-team for irradiation.

## Irradiation, Measurement, Analysis

The prepared samples are now irradiated in the reactor for one hour with a neutron flux of  $10^{13} \text{ cm}^{-2} \text{ s}^{-1}$ . According to the half-life of  $^{42}\text{K}$  (12.361 h), the samples have to be decayed for about 12 to 16 hours. The dose rate of the irradiation capsule is checked and if it does not exceed a set limit it is brought back to the laboratory where it is opened and the polyethylene casings are cleaned in consideration of safety measures. After that the samples are measured for 600 s via  $\gamma$ -spectroscopy. Each received peak refers to the  $\gamma$ -energy of an element or isotope in the sample. For  $^{42}\text{K}$  its characteristic energy is 1525 eV and the peak is shown in Fig. 3.2.

Sample Date :		Chi-square : 1.98				
Fit Engine : Sum / Non-Linear LSQ Fit		Region Start : 1520.730 keV				
Bkgnd Type : Step		Region End : 1529.275 keV				
Nbr	Energy	Centroid	Area	%Error	FWHM	Ratio
1	1525.08	3926.22	25916.81	1.42	2.261	1.04

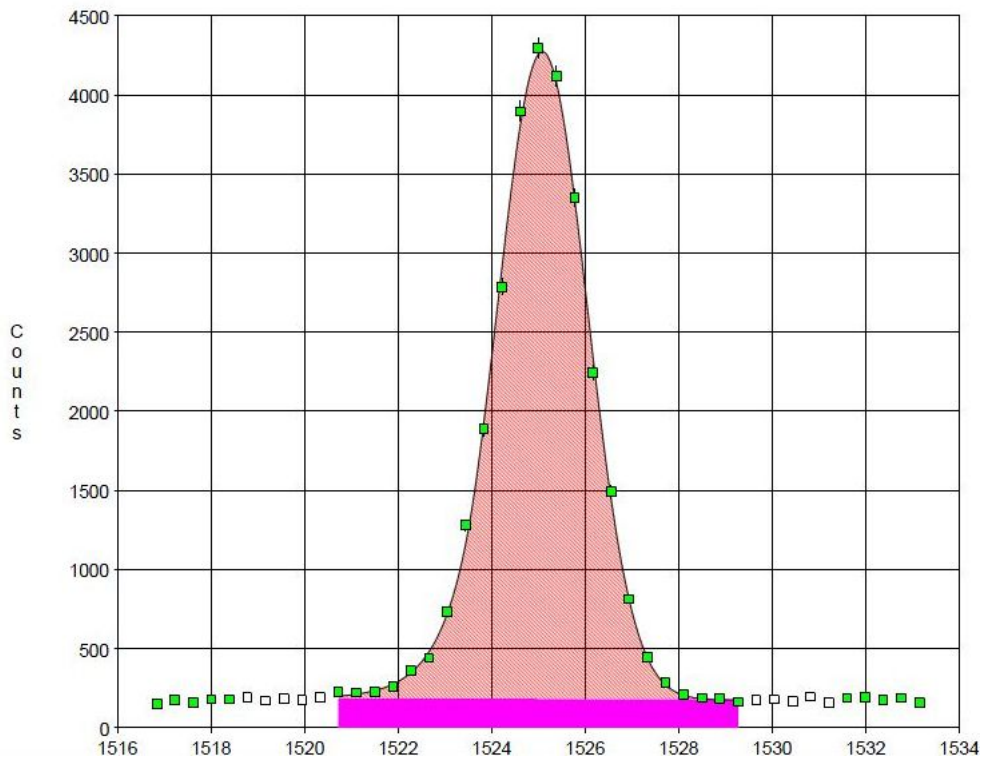


Figure 3.2:  $^{42}\text{K}$  peak of PBP2 in  $\gamma$ -spectroscopy after neutron activation analysis

The peak area is directly proportional to the concentration of the element. In comparison with the standard material, the potassium concentration in the sample can be determined.

The activity of an element is given by

$$\begin{aligned} A(t) &= \lambda N(t) = -\frac{dN(t)}{dt} \\ &= A_0 \cdot e^{-\lambda t} \end{aligned} \quad (3.5)$$

$A(t)$ ...activity at t [Counts/s]  
 $N(t)$ ...number of particles at t [Counts],  $N(t) = N_0 \cdot e^{-\lambda t}$   
 $A_0$ .....activity at t=0 [Counts/s],  $A_0 = N_0 \lambda$   
 $N_0$ .....number of particles at t=0 [Counts]  
 $\lambda$ .....decay constant [1/s],  $\lambda = \frac{\ln(2)}{T_{1/2}}$   
 $T_{\frac{1}{2}}$ .....half-life [s]

Applying that to the given situation

$$A_t = \frac{N}{T} = A_0 \cdot e^{-\lambda T_D} \quad (3.6)$$

$A_t$ ...activity at end of measurement [Counts/s]  
 $A_0$ ...activity at start of measurement [Counts/s]  
 $N$ ....peak area of sample [Counts]  
 $T$ ....testing time  
 $\lambda$ .....decay constant [1/s]  
 $T_{\frac{1}{2}}$ ...half-life [s],  $T_{\frac{1}{2}}(^{42}\text{K}) = 12.361 \text{ h}$   
 $T_D$ ...time difference between standard and sample measurement [s]

and considering the time difference between measurements and the masses of the sample and the standard

$$\frac{C_s}{C_{st}} = \frac{\frac{A_s}{m_s \cdot e^{-\lambda T_D}}}{\frac{A_{st}}{m_{st}}} \quad (3.7)$$

the concentration of potassium in the sample can be obtained by

$$C_s = C_{st} \cdot \left( \frac{A_s \cdot e^{\lambda T_D} \cdot T_{st} \cdot m_{st}}{A_{st} \cdot T_s \cdot m_s} \right). \quad (3.8)$$

$C_s$ ....potassium concentration of sample [%]  
 $C_{st}$ ...potassium concentration of standard [%]  
 $A_s$ ....peak area of sample [Counts]  
 $A_{st}$ ...peak area of standard [Counts]  
 $T_s$ .....testing time of sample [s]  
 $T_{st}$ ....testing time of standard[s]  
 $m_s$ ....mass of sample [mg]  
 $m_{st}$ ...mass of standard [mg]  
 $\lambda$ .....decay constant [1/s]  
 $T_D$ ....lag between standard and sample measurement [s]

while using the values of the analysis sheet, received as a result of the measurement (eg. Fig. 3.3). In addition, the potassium oxide concentration has to be determined. As 1 g potassium oxide contains 0.830 g potassium the conversion factor is 1.205.

These formulas are integrated in the program module described in section 3.3.3.

```

*****
A n a l y s i s  s h e e t
*****

Sample Title:                               4, P2, 18S, 86mg

Acquisition Start Time: 10.11.09 08:38:00
Live Time:              600 seconds
Real Time:              600 seconds

Peak Analysis Performed: 10.11.2009 09:31:17
Analysis from channel:   1
Analysis to channel:     8192


```

Peak No.	Energy [keV]	Net Peak Area[cts]	Bkgnd [cts]	FWHM [keV]	Counts/sec	Error [%]
F 1	60.71	3216	28691	2.203	5.360E+000	5.33
M 2	69.49	2503	27029	1.305	4.172E+000	5.19
M 3	72.72	17801	29410	1.312	2.967E+001	1.04
M 4	75.02	27487	26891	1.317	4.581E+001	0.79
M 5	84.64	15308	28907	1.401	2.551E+001	1.24
M 6	87.19	4845	28230	1.406	8.075E+000	2.95
F 7	102.96	4085	30641	1.144	6.809E+000	3.61
F 8	121.52	8189	30397	1.197	1.365E+001	1.99
F 9	133.93	5795	30547	1.186	9.658E+000	2.69
F 10	312.34	1040	29261	1.353	1.733E+000	12.92
F 11	328.31	1792	18057	1.264	2.987E+000	7.12
F 12	343.97	1906	22637	1.564	3.177E+000	7.08
M 13	479.06	8248	12248	1.546	1.375E+001	1.61
M 14	486.57	3351	12166	1.552	5.585E+000	3.08
F 15	510.57	77757	17420	2.663	1.296E+002	1.04
M 16	551.11	1542	9793	1.440	2.570E+000	5.96
M 17	558.71	1207	10102	1.446	2.012E+000	7.29
F 18	617.82	1982	14958	1.855	3.303E+000	5.40
F 19	629.62	678	14034	1.440	1.120E+000	13.50
F 20	685.30	7515	12101	1.595	1.252E+001	1.64
F 21	772.41	810	9007	1.422	1.350E+000	10.15
F 22	815.28	1209	10779	1.781	2.014E+000	7.61
M 23	832.70	2740	10103	1.798	4.566E+000	3.28
M 24	841.12	6001	10687	1.803	1.000E+001	1.97
M 25	846.34	48213	10599	1.806	7.202E+001	1.10
F 26	963.05	4689	12242	1.916	7.815E+000	7.28
F 27	1368.82	279827	6579	2.181	4.664E+002	0.34
<b>F 28</b>	<b>1525.09</b>	<b>25917</b>	<b>4132</b>	<b>2.261</b>	<b>4.319E+001</b>	<b>1.42</b>
F 29	1596.83	2980	3725	1.869	4.967E+000	1.93
F 30	1732.47	18863	4656	2.576	3.144E+001	1.73
F 31	2114.42	3035	5488	2.236	5.059E+000	2.10
F 32	2244.18	25578	7649	3.593	4.263E+001	1.81
F 33	2755.86	153758	2840	3.034	2.563E+002	0.50

Errors quoted at 1.00 sigma

Figure 3.3: Analysis sheet of sample PBP2

### 3.1.4 External $\gamma$ -Dose Rate and Cosmic Dose Rate

The external  $\gamma$ -dose rate can be determined as shown in section 2.9.4. Another possibility to obtain the dose rates is to consult special radiation maps. The cosmic dose rate can also be looked up in radiation maps or can be calculated by (Prescott and Stephan, 1982) [6]

$$I(h) = K \left[ F + J \cdot e^{\frac{h}{H}} \right]. \quad (3.9)$$

$I(h)$ .....cosmic dose rate [mGy/a]  
 $h$ .....sea level of excavation site [m]  
 $K$ .....constant:  $0.185 \pm 0.011$  [mGy/a]  
 $F, J, H$ [km]...slowly varying functions of latitude (readable in Fig. 3.4)

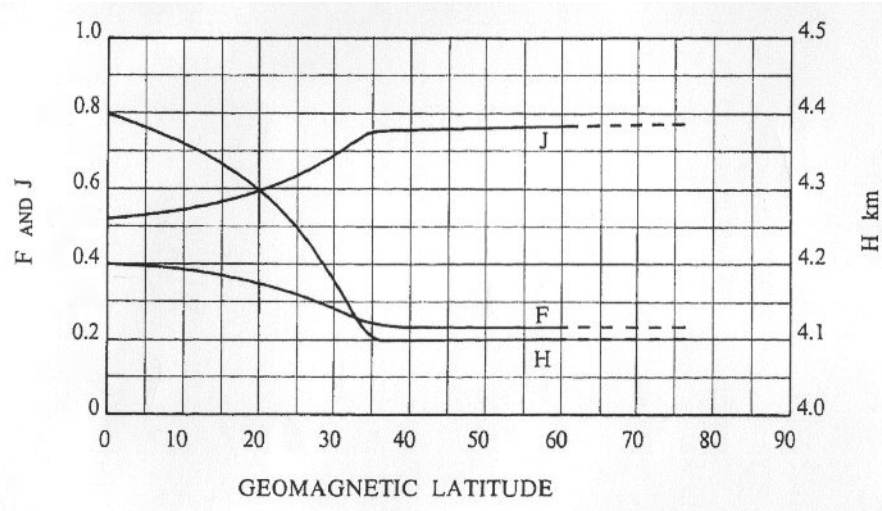


Figure 3.4: Parameters in equation (3.9) by Prescott and Stephan (1982) [6]

In order to obtain the parameters F, J and H the geomagnetic latitude  $\lambda$  has to be determined by

$$\lambda = \arcsin(0.203 \cdot \cos\vartheta \cdot \cos(\varphi - 291) + 0.979 \cdot \sin\vartheta). \quad (3.10)$$

$\vartheta$ ...geographic latitude (north latitudes are positive)  
 $\varphi$ ...geographic longitude (east longitudes are positive)

## 3.2 Sample Preparation

The objective of the preparation is that approximately 1.5 - 1.8 mg sample powder with a grain size of 1 to 8  $\mu\text{m}$  is obtained. At first, aluminium disks (10 mm  $\varnothing$ ) have to be homogenously coated with the powder and measured with the thermoluminescence device. The whole procedure (Bergmann, 2005) [18] has to be performed under red light, as white light would empty the electron traps and thereby affect the measurement.

### 3.2.1 Preparation

- It has to be checked whether enough pure acetone, distilled water and 5 %-acetic acid is at hand.
- The drill, the mortar, the spatula, two test tubes, two beakers (100 and 200 ml), the pipette and the tweezer have to be cleaned and some speckless sheets of paper have to be used as underlay. The 200 ml-beaker and the test tubes have to be marked at 6 cm.
- The aluminium stands (Primerano, 1999) [21] and disks have to be cleaned as follows:
  - The stands (with their holes pointing downwards) are held into the ultrasonic bath for five minutes and the air inside is let out by tilting.
  - Afterwards the stands are washed with supply water and held in the ultrasonic bath again. This time the openings look up but must not be flooded by water. They are filled with acetone and left there for another 5 minutes.
  - Finally they are taken out, the acetone is removed and the stand is additionally cleaned with cotton buds.
  - The aluminium disks are likewise cleaned with acetone in the ultrasonic bath and can be wiped with paper towels afterwards.

### 3.2.2 Drilling

The rotational speed of the drill has to be kept low to avoid the emptying of the electron traps due to heat. Firstly, a homogenous area of the sample is chosen as inclusions may affect the results. Furthermore, the obtained powder should not encounter the surface of the sample because it could be polluted. Having chosen such a spot and made all the preparations the drilling can be started.

At first 2 mm of the surface are removed in order to get the powder where no optical stimulation had taken place and the absorption of  $\alpha$ - and  $\beta$ -radiation can be



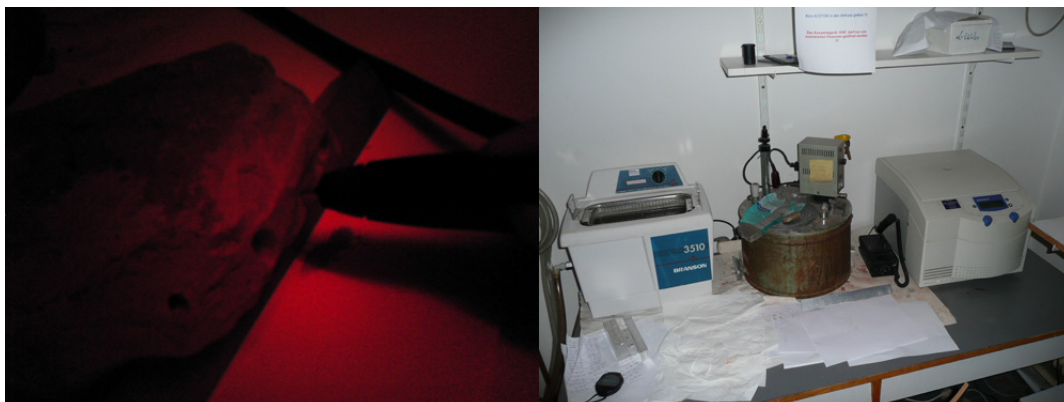


Figure 3.5: Drilling under red light, desk space for drilling and ultrasonic bath

neglected. The powder obtained by drilling the 2 mm of surface can be used for determination of the  $\alpha$ -counting rate whereupon more material is needed. Eventually, the further accrued powder is gathered on a clean sheet of paper. Depending on the grain size, the dimension of the sample and its preciousness more or less powder is drilled, but as a guideline 40 mg should be enough for an age determination. The powder can be fractionated or ground to decrease the grain sizes.

### 3.2.3 Grinding

The appliance of grinding is another method to obtain powder of the sample. The yield of this procedure is higher than the yield of drilling. The heat produced by grinding is however lower than that occurring during drilling.

At first 2 mm of the surface have to be removed in order to neglect optical stimulation and the influence of the surrounding  $\alpha$ - and  $\beta$ -radiation. Then little slivers are separated by means of hammer and chisel. The fragments are pulverized in a mortar, the powder is filled into a test tube and can now be fractionated.

### 3.2.4 Fractionation

Fractionation is based on the Stokes' law on falling bodies and goes for separation of grain sizes.

1. At first the test tube with the sample powder is filled with acetone up to the 6 cm-marking. It has to rest for 2 minutes and afterwards the acetone is decanted into the 200 ml-beaker without admixing the sediment as it contains particles with grain sizes larger than 8  $\mu\text{m}$ . The procedure is repeated





Figure 3.6: Desk space for fractionating, oven

until the 6 cm-marking of the beaker is reached. The mixture is stirred and allowed to stand for 20 minutes.

2. When the time has passed the acetone is decanted and working with the sediment can be continued. Some acetone is filled into the beaker and the sediment is loosened in an ultrasonic bath for 2 to 3 minutes. The whole mixture is decanted into another test tube which is filled with acetone up to the 6 cm-marking. The sample is centrifugated for 2 to 3 minutes and the acetone is decanted again.
3. Afterwards the test tube is filled approximately 1 cm high with 5 %-acetic acid and held into an ultrasonic bath for 10 minutes to purify and loosen the grains. Then the sample is centrifugated for 2 to 3 minutes and the acetic acid is decanted.
4. To eliminate the acetic acid from the sample and to avoid chemiluminescence the following procedure is repeated twice: The test tube is filled with distilled water up to the 6 cm-marking and then the grains are loosened in an ultrasonic bath for 2 to 3 minutes and centrifugated for 2 to 3 minutes. The distilled water is removed.
5. Additionally step 4 is repeated twice but with acetone instead of distilled water.
6. Finally the test tube is filled with acetone up to the 6 cm-marking, the mixture is stirred and allowed to stand for another 20 minutes so that grains smaller than 1  $\mu\text{m}$  which were formed during the acetic acid-cycle can be separated.

7. The acetone is decanted without the sediment and the test tube is put into the oven over night at 40 °C.

### **3.2.5 Sedimentation**

The aluminium stands which were used for sedimentation as well as the exact procedure were developed by Primerano (1999) [21].

1. After drying a light-proof case is weighed, at first without and then with the sample to obtain its net weight. The amount of needed aluminium disks depending on the coating can be determined.
2. The aluminium stands are placed on a table and an aluminium disk is put in each opening. 1 ml of acetone is divided and pipetted in 3 openings to moisten the disks.
3. The sample powder within the test tube obtained by fractionation (1-8 µm) is loosened with 1 ml acetone and decanted into the 100 ml-beaker. As much acetone, as needed for pipetting 1.5 to 1.8 mg of the sample with 1 ml of the dilution, is added.
4. Afterwards the dilution is intermixed in the ultrasonic bath until no more sediment is recognizable.
5. Thereafter it is carefully pipetted into the openings and the beaker is held into the ultrasonic bath after pipetting approximately 3 disks in order to avoid forming a sediment.
6. The stands with the dilution are allowed to stand for 20 minutes and then they are put into the oven over night at a temperature of 40 °C.
7. After dehumidifying the stands are tilted out a clean sheet of paper and the disks with the sample powder on them are sorted in a light-proof briefcase.

## **3.3 Measurement**

### **3.3.1 HVK-Device**

The thermoluminescence device by which the measurement of the prepared samples is carried out was developed by Henzinger (1993) [22] along with Vana and Kubelik at the Institute of Atomic and Subatomic Physics in Vienna. It is therefore briefly called “HVK” and includes

- a vacuum-sealed metering chamber



Figure 3.7: HVK-device, device controlling computer (left) and data analyzing computer (right)

- a computer with a control program
- a vacuum pump
- a pressure cylinder with ultrapure nitrogen
- a photomultiplier (EMI 9235QA) with a filter (Schott UG-11)
- a heating system
- an  $\alpha$ - and a  $\beta$ -source ( $^{241}\text{Am}$  ( $T_{\frac{1}{2}} = 433 \text{ a}$ ),  $^{90}\text{Sr}$  ( $T_{\frac{1}{2}} = 28 \text{ a}$ )) for irradiation
- and a turntable for 60 samples.

At first the chamber is evacuated and flooded with pure nitrogen in order to reduce modified luminescence occurring due to water vapour during the heating process (see section 2.5.3). Then the samples are pre-heated at 190 °C for a minute one after the other to dissipate unstable traps (see section 2.5.4), and are heated with 5 °C per second up to 500 °C. The irradiation with the  $\alpha$ - and  $\beta$ -sources for previously selected samples is carried out automatically and afterwards the emitted photons of the once more heated sample are detected by the photomultiplier.

### 3.3.2 Measuring Sequence

The HVK-device is powered and necessary parameters are registered in the control program (amount of measured samples, the heating interval, kind of irradi-

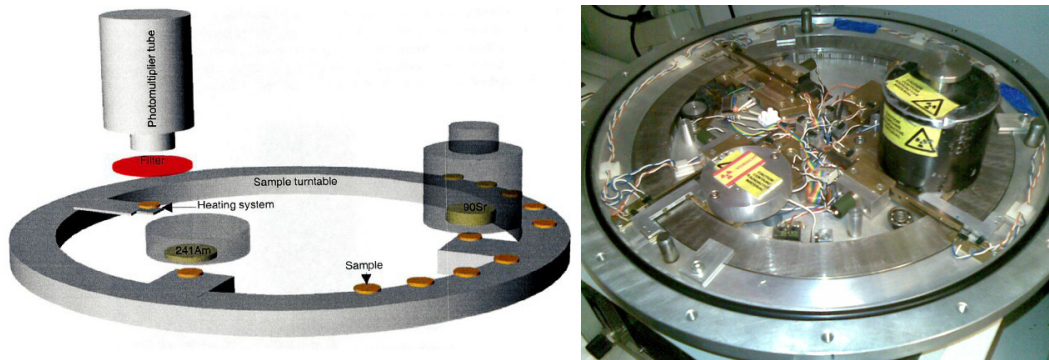


Figure 3.8: Schematic diagram of the HVK (Tatlisu, 1999) [7], opened HVK-device

ation, period of irradiation,...). The samples are placed in the metering chamber and the measurement process is started.

One usually begins with up to four samples. The natural thermoluminescence of two of them is measured, that means they are not irradiated additionally. One sample is then irradiated with the  $\beta$ -source for five and the other one for ten minutes in order to obtain the second-glow-curves by reheating so the intercept can be determined. The remaining two samples are irradiated with the  $\beta$ -source with 1.98 Gy ( $\cong$  5 min, in October 2009) and 3.96 Gy ( $\cong$  10 min, in October 2009) respectively and heated again. So the glow-curves with the natural plus the particular dose are obtained. After estimating the age of the sample with this data, it can be decided what kind and duration of irradiation shall be used for measuring the rest of the available disks. The accuracy of the process is increased the more samples are measured. After each cycle the data are stored on a disk and transferred to a computer with an analysis program where the age of the sample can be determined. The software was developed and renewed by Gratzl (1989) [17] and was enhanced by including the age calculation-program module in the course of this master thesis which has several new features. The renewed version of the software consists of:

- Glow-curve window:  
The glow-curves are displayed and diverse features can be executed (subtraction of curves, plateau test, zoom, smoothing, correlation, integration,...).
- EAI window(Equivalent dose, Alpha-equivalent dose, Intercept):  
3 regression lines are displayed. Every reading point can be selected or de-selected and the  $\alpha$ - and  $\beta$ -equivalent doses and the intercept are determined along with their standard deviations.

- Age calculation window:  
The  $\alpha$ - and  $\beta$ -equivalent doses and the intercept along with their standard deviations are automatically transferred from the EAI window or can be entered manually and thereby the  $\alpha$ -efficiency is determined.

Following parameters can be calculated with this program module or registered:

- $\alpha$ -counting rate (amount of counted  $\alpha$ -particles/ks)
- pairs rate (amount of coincidence pairs/ks)
- saturation weight increase
- saturation fraction
- $K_2O$ -contents
- cosmic dose rate
- external  $\gamma$ -dose rate
- self-dose percentage by entering form and thickness of sample
- error caused by stony surroundings

Following results are obtained:

- breakdown of the total dose rate in  $\alpha$ -,  $\beta$ - and  $\gamma$ -proportions.
- random, systematic and total error
- age of the sample and the deviation thereof

Furthermore a printout of this data can be made. The formulas of sections 2.9 and 2.10 are included and used for this program module which is specified in section 3.3.3.

Subsequently the further processing of the data and its analysis is described.

Fig. 3.9 shows a natural glow-curve (blue) which was obtained by heating the sample with a constant heating rate of 5 °C per second up to 500 °C without additional irradiation. The emitted photons are detected by the photomultiplier and hence the measured thermoluminescence against the heating temperature is displayed. It has to be taken into account that this so obtained glow-curve does not only consist of the thermoluminescence signal but also of spurious thermoluminescence, which contains the dark current of the photomultiplier, the black-body radiation, which is commensurate to  $T^4$  and dominates from approximately

400 °C upwards, and some other chemical and triboluminescence effects. The two occurring effects mentioned above are added up and represent the so-called background which can be determined by reheating the sample with the same heating rate (black). By subtracting the background from the glow-curve the curve with consisting only of the thermoluminescence signal (red) is obtained.

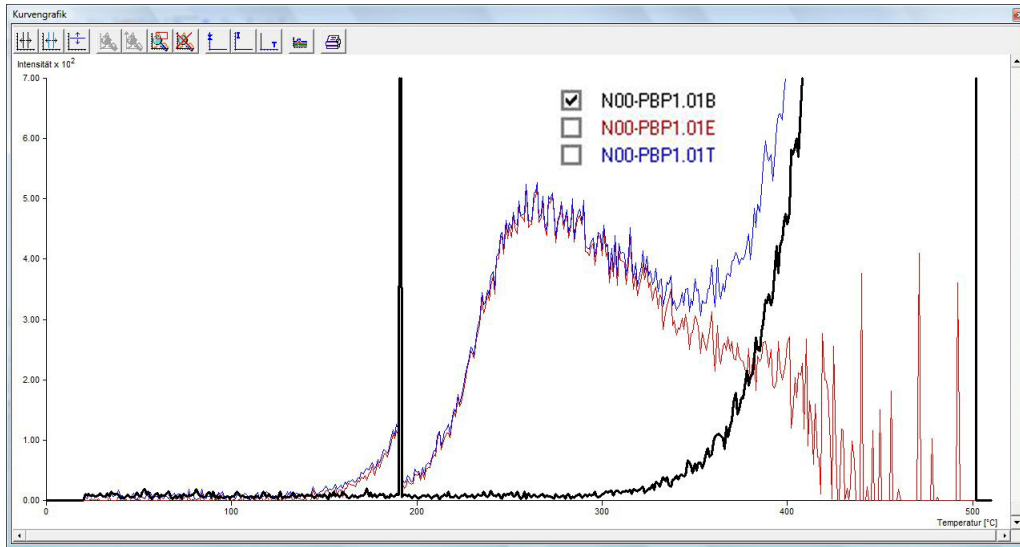


Figure 3.9: Natural glow-curve

Moreover the samples are irradiated with different doses and measured. The used doses are known and according to them the obtained glow-curves are higher than the natural ones. Fig. 3.10 shows natural (N00) and  $\beta$ -irradiated ( $N\beta1 \cong 1.98$  Gy,  $N\beta2 \cong 3.96$  Gy,  $N\beta3 \cong 5.93$  Gy,  $N\beta4 \cong 7.91$  Gy) glow-curves.

In order to get a suitable analysis area the plateau test is applied as described in section 2.6. As it determines the ratio of natural to artificially irradiated samples it helps finding a adequate integration area. Fig. 3.11 shows the plateau test of the glow-curves of three  $\beta$ -irradiated samples with a natural one.

The area in which the values of the glow-curve are constant is called plateau and the included interval which is chosen is without large fluctuations. Fig. 3.12 shows such an area between 276 °C and 304 °C.

After integrating the glow-curves in this interval the results are displayed in a coordinate system with the x-coordinate describing the additional doses and the y-coordinate the integration values. Through these dots a line is plotted and so the regression lines for the different kinds of irradiation are obtained as shown in Fig. 3.13.

Hence, the  $\beta$ -equivalent dose is received by determining the intersection of the  $\beta$ -regression line (black) with the x-axis whereas the  $\alpha$ -equivalent dose is



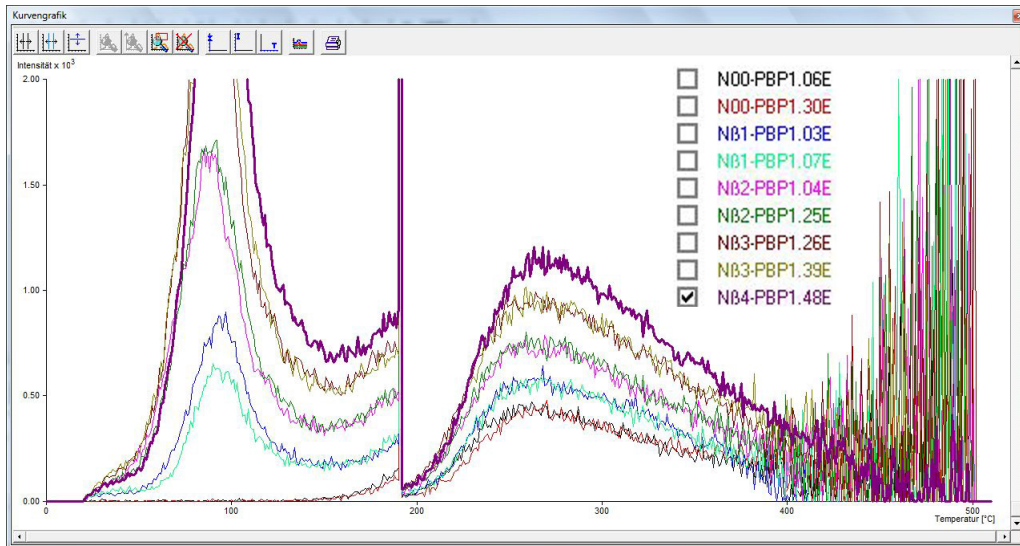


Figure 3.10: Natural and artificially  $\beta$ -irradiated glow-curves

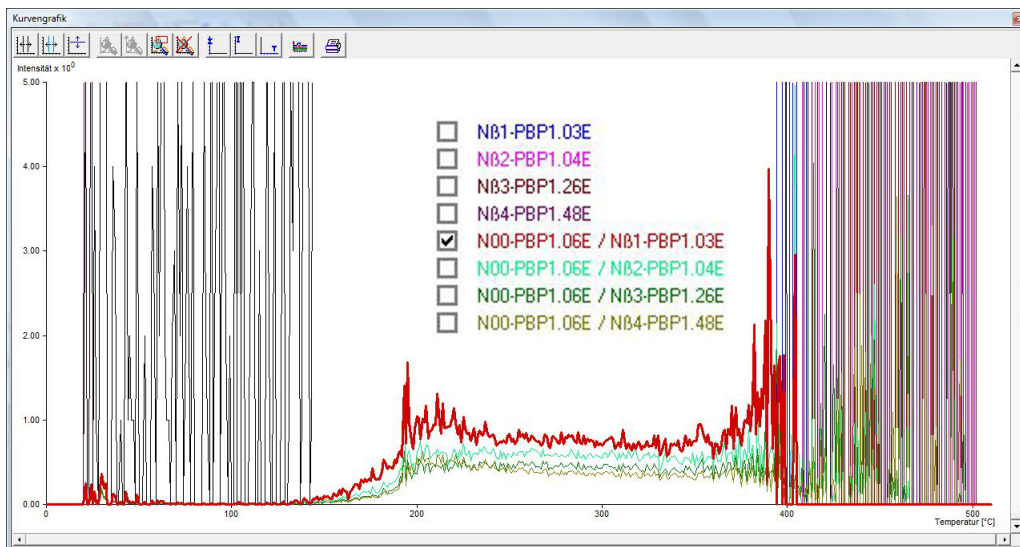


Figure 3.11: Plateau test

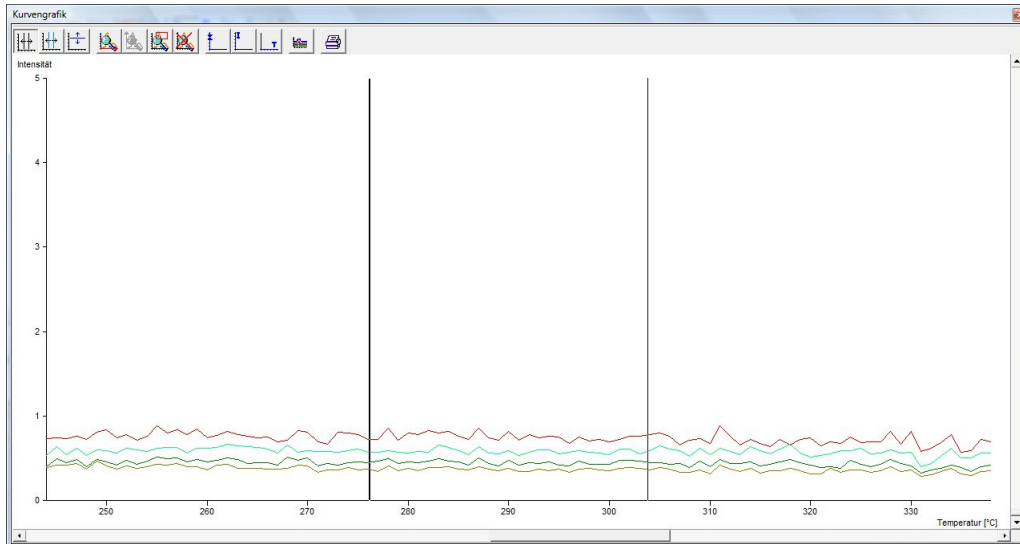


Figure 3.12: Zoomed integration interval

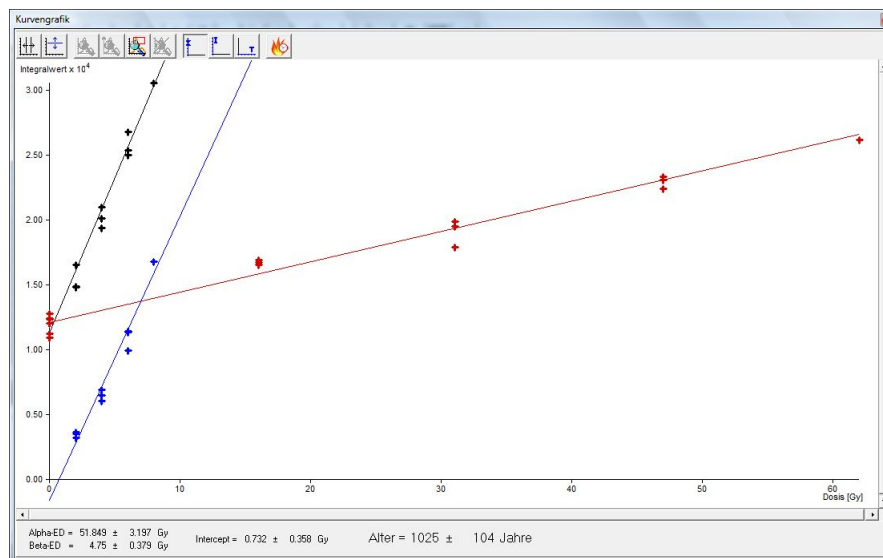


Figure 3.13: Regression lines



obtained by determining the intersection of the  $\alpha$ -regression line (red) with the x-axis. The intercept is ascertained in order to consider the supralinearity since there is no linear connection between the absorbed dose and the thermoluminescence at small doses. For the purpose of determining the intercept the samples which have been measured once are again irradiated by the  $\beta$ -source for different time periods and measured to receive the second-glow-curves. Consequently the second-glow-curve regression line can be obtained analogously as mentioned above and the deviation of the linearity, the intercept, is the distance between the origin and the intersection of the second-glow-regression line (blue) with the x-axis. In addition, if the parallelity of the  $\beta$ - and the second-glow-regression line is observable it shows equal sensitivity and well chosen integration intervals. The received values of the  $\alpha$ - and  $\beta$ -equivalent doses and the intercept are transferred into the age calculation-program module, which is described in the next section 3.3.3, where the age of the sample is determined after entering the additionally necessary parameters.

### 3.3.3 Age Calculation-Program Module

The module consists of eight units and Delphi 6.0 was used as programming language. Parameters are displayed and can be modified separately in order to display the effects on the calculated age. Furthermore, shortcuts can be used for eg. loading, saving, printing and so on.

#### Concept of the User Interface

- selection via input windows
- input by using mouse or keyboard
- every value just needs to be entered once

#### Age Calculation Unit

In this dialog parameters are entered to determine the age of the sample. Hence the calculation of the age of the sample and the estimation of the age determination errors take place.

Each parameter set can be saved in a text file for further utilization. On opening the program module average default values (reasonable values) are predefined in order to get a raw estimation of the age of the sample as shown in Fig. 3.14.

Figure 3.14: Age Calculation dialog

### Parameters:

- $Q_{\alpha} \pm dQ_{\alpha}$  [Gy]:  $\alpha$ -equivalent dose and its standard deviation
- $Q_{\beta} \pm dQ_{\beta}$  [Gy]:  $\beta$ -equivalent dose and its standard deviation
- $I \pm dI$  [Gy]: Intercept and its standard deviation
- $A \pm dA$  [Gy]:  $\alpha$ -efficiency and its standard deviation
- **$\alpha$ -counting rate [counts/ks]:** amount of counted  $\alpha$ -particles using the  $\alpha$ -counter (screen 42 mm  $\varnothing$ ); can be calculated by pressing the button “Calculate Alpha-Counting Rate” as shown in section 3.3.3
- **Pairs rate [counts/ks]:** amount of coincidence pairs ( $\alpha$ -counter with pair detection), has to be set to “–1” if the value has not been determined; can be calculated by pressing the button “Calculate Alpha-Counting Rate” as shown in section 3.3.3
- **Saturation weight increase (W):** increase of weight when water content is saturated.  
This value has to be entered as proportion ( $0.2 \hat{=} 20\%$ ) or can be calculated

by pressing the button “Calculate Values” as shown in section 3.3.3. The deviation of the saturation weight increase is not calculated because the effect on the total systematic error would increase maximally by 5 % and the total error would be raised by maximally 0.1 %. Therefore, the deviation is negligible in age determination.

- **Saturation fraction (F), dF:** Wetness and its deviation; the values have to be entered as proportion; F can be calculated by pressing the button “Calculate Values” as shown in section 3.3.3. dF is not calculated because the effect on the total systematic error would increase maximally by 5 % and the total error would be raised by maximally 0.1 %. Therefore, the deviation is negligible in age determination.
- **Effective  $\alpha$ -dose rate [mGy/a]:** total, calculated annual effective  $\alpha$ -dose rate within the sample
- **$\beta$ -attenuation:** 0.9 for inclusion dating, 1 for fine-grain dating
- **$K_2O$ —Contents [W %]:** weight percentage of potassium oxide; can be calculated by pressing the button “Calculate Potassium Oxide-Contents” as shown in section 3.3.3. The deviation of the  $K_2O$ —contents is not calculated because the effect on the total systematic error would increase maximally by 5 % and the total error would be raised by maximally 0.1 %. Therefore, the deviation is negligible in age determination.
- **$\beta$ -dose rate [mGy/a]:** total, calculated annual  $\beta$ -dose rate within the sample
- **Internal  $\gamma$ -dose rate [mGy/a]:** consists of a thorium/uranium and potassium component
- **External  $\gamma$ -dose rate [mGy/a]:** corrected (wetness, cosmic dose rate), measured annual  $\gamma$ -dose rate of soil and its error or read out of radiation maps; can be calculated by pressing the button “Calculate External  $\gamma$ -Dose Rate” as shown in section 3.3.3
- **Sample shape:** shape of the sample for calculating the self-dose percentage; it can be chosen between flat or spheric
- **Sample thickness [cm]:** thickness of the sample for calculating the self-dose percentage
- **$\gamma$ -dose rate [mGy/a]:** total annual  $\gamma$ -dose rate within the sample

- **Saturation weight increase of soil:** increase of the weight of soil when water content is saturated, used for the calculation of the external  $\gamma$ -dose rate and the calculation of the error in age due to wetness fraction; the value has to be entered as proportion
- **Cosmic dose rate [mGy/a]:** annual cosmic dose rate, can be calculated by pressing the button “Calculate Cosmic Dose Rate” as shown in section 3.3.3
- **Total dose rate [mGy/a]:** total annual dose rate consisting of the  $\alpha$ -,  $\beta$ -,  $\gamma$ - and cosmic dose rates; the particular percentages are shown

#### Errors:

- **TL measurement:** error due to the standard deviations of  $Q_\alpha$ ,  $Q_\beta$  and I
- **Annual dose:** error due to determination of the annual doses
- **Stone content:** error due to the surroundings of the sample while buried; can be calculated by pressing the button “Error Stone Content” as shown in section 3.3.3
- **Total random error:** total calculated random error, all random errors have been considered
- **Calibration:** systematic error arising from calibration
- **Th/U-ratio:** error estimation due to not-determining the pairs rate, “-1” has to be registered in the pairs rate-input field in order to start the error calculation
- **Wetness fraction:** error because of the deviation of the saturation fraction
- **Total systematic error:** total calculated systematic error; all systematic errors have been considered
- **Total error:** total calculated error (total error of the age of the sample); the total random error and the total systematic error have been considered

#### Commands:

- **OK:** initializes all calculations and allows the return to the main program with transferring the data
- **Execute:** initializes all calculations

- **Cancel:** allows the return to the main program without transferring the data
- **Load:** the currently shown parameter set and the age and calculated error can be loaded from a text file
- **Save:** the currently shown parameter set and the age and calculated error can be saved to a text file
- **Print:** the currently shown parameter set and the age and calculated error can be printed
- **Default Values:** resets the parameters
- **E:** the language of the whole user interface is changed to English
- **DE:** the language of the whole user interface is changed to German
- **Help:** currently not available

## Programming

The inherited and entered parameters are read in in the procedure *CalcAge* as shown in Lst. 1 in lines 7 to 26 and hence the determination of the age of the sample and its error take place as well in the same procedure. Calculations base upon the formulas in section 2.9 and 2.10.

```

1  procedure TFormAge.CalcAge(VAR Age : REAL; VAR dAge : REAL);
2  var p : Real;
3      Error : Boolean;
4      Origin : Integer;
5  begin
6      Error := False;
7      p := StrToFloat(Labelp.Caption);
8
9      Qa          := StrToFloat(EditQa.Text);
10     dQa          := StrToFloat(EditdQa.Text);
11     Qb           := StrToFloat(EditQb.Text);
12     dQb          := StrToFloat(EditdQb.Text);
13     Intercept    := StrToFloat(EditI.Text);
14     dIntercept   := StrToFloat(EditdIntercept.Text);
15
16     bAttenuation := StrToFloat(LabelbAttenuation.Caption);
17     dF           := StrToFloat(EditdF.Text);
18     try
19         K2O       := StrToFloat(EditK2O.Text);
20     except
21         Error := True;
22         K2O := 0;
23         EditK2O.Text := '0';
24     end;
25

```

```

26 ...//the rest of the parameters are read in in an analogous manner
27 //(pairsrate, aCountrate, W, F, Ws, DgExt, Dk)
28
29 if Error then begin
30   if FormAge.BitBtnGerman.Enabled then Showmessage('Check Entries!')
31   else Showmessage('Eingaben berpr fen!')
32   end
33 else
34   if (Qa > 0) then
35     begin
36       aEfficiency := Qb/Qa;
37       EditA.Text := FloatToStr(Round(1000*aEfficiency)/1000);
38       daEfficiency := (Qa*dQb-Qb*dQa)/Power(Qa,2);
39       EditdAlphaEfficiency.Text := FloatToStr(Round(1000*daEfficiency)/1000);
40
41       if Pairsrate > -0.1 then begin
42         AThorium := 21*(Pairsrate - 0.38*Power(aCountrate,2)/1000);
43         AUran := aCountrate-AThorium;
44         Da := aEfficiency*(1.2728*AThorium+1.2792*AUran)/(1+1.5*W*F);
45         DbThU := bAttenuation*(0.057*AThorium+0.087*AUran)/(1+1.25*W*F);
46         DgIntThU := (0.103*AThorium+0.068*AUran)/(1+1.14*W*F);
47       end
48
49       else begin
50         Da := aEfficiency*1.276*aCountrate/(1+1.5*W*F);
51         DbThU := bAttenuation*0.072*aCountrate/(1+1.25*W*F);
52         DgIntThU := 0.085*aCountrate/(1+1.14*W*F);
53
54       end;
55
56       DbKRb := bAttenuation*0.708*K2O/(1+1.25*W*F);
57       Db := DbThU + DbKRb;
58       DgIntK := 0.241*K2O/(1+1.14*W*F);
59       DgInt := DgIntThU+DgIntK;
60       Dg := p/100*DgInt+(1-p/100)*DgExt;
61       Dtotal := Da+Db+Dg+Dk;
62       EditDa.Text := FloatToStr(Round(1000*Da)/1000);
63       EditDb.Text := FloatToStr(Round(1000*Db)/1000);
64       EditDgInt.Text := FloatToStr(Round(1000*DgInt)/1000);
65       EditDg.Text := FloatToStr(Round(1000*Dg)/1000);
66
67       if RadioButtonFineGrain.Checked then
68         Age := (Qb+Intercept)/((Da+Db+Dg+Dk)/1000)
69       else
70         Age := (Qb+Intercept)/((0.9*Db+Dg+Dk)/1000);
71       LabelAge.Caption := FloatToStr(round(Age));
72
73       fa := Da/Dtotal;
74       fb := Db/Dtotal;
75       fg := Dg/Dtotal;
76       fk := Dk/Dtotal;
77       fbThU := DbThU/Dtotal;
78       fbKRb := DbKRb/Dtotal;
79       fgIntThU := p/100*DgIntThU/Dtotal;
80       fgIntK := p/100*DgIntK/Dtotal;
81       fgInt := p/100*DgInt/Dtotal;
82       fgExt := (1-p/100)*DgExt/Dtotal;
83
84       sig1 := sqrt(sqrt(100*(1-fa*(Qb+Intercept)/Qb)*dQb/(Qb+Intercept))
85             +sqrt(100*dIntercept/(Qb+Intercept))+sqrt(100*fa*dQa/Qa));
86       LabelTLMeasurement.Caption := FloatToStr(Round(100*sig1)/100);
87

```

```

88      sig2:= sqrt(25*(sqr(fa+fbThU+fgIntThU)+sqr(fbKRb+fgIntK)+sqr(fgExt)));
89      LabelAnnualDose.Caption := FloatToStr(Round(100*sig2)/100);
90
91      sig3 := StrToFloat(LabelStoneContent.Caption);
92
93      sig4 :=sqrt(25*(sqr(fa)+sqr(1-fa)+sqr(fa+fbThU+fgIntThU)
94                +sqr(fbKRb+fgIntK)+sqr(fgExt)));
95      LabelCalibration.Caption := FloatToStr(Round(100*sig4)/100);
96
97      if Pairsrate > -0.1 then sig5:=0
98      else sig5:=14*abs(fbThU-fgIntThU);
99      LabelThURatio.Caption := FloatToStr(Round(100*sig5)/100);
100
101      sig6:=100*(1.5*fa*W+1.25*fb*W+1.14*fgInt*W+1.14*fgExt*Ws)*df;
102      LabelWetness.Caption := FloatToStr(Round(100*sig6)/100);
103
104      sigstat:=sqrt(sqr(sig1)+sqr(sig2)+sqr(sig3));
105      sigsys:=sqrt(sqr(sig4)+sqr(sig5)+sqr(sig6));
106      sigtotal:=sqrt(sqr(sigstat)+sqr(sigsys));
107
108      LabelErrorRandom.Caption := FloatToStr(Round(100*sigstat)/100);
109      LabelErrorSys.Caption := FloatToStr(Round(100*sigsys)/100);
110      LabelErrorTotal.Caption := FloatToStr(Round(100*sigtotal)/100);
111
112      dAge:=Age/100*sigtotal;
113      LabeldAge.Caption := FloatToStr(Round(dAge));
114
115      Origin := StrToInt(FormatDateTime('yyyy', Now))-
116                StrToInt(LabelAge.Caption);
117      LabelDate.Caption := '('+IntToStr(Abs(Origin));
118      if Origin > 0 then LabelC.Caption := 'a.c.)'
119      else LabelC.Caption := 'b.c.)'
120  end;
121 end;

```

Listing 1: Procedure *CalcAge* manages the calculation of the age of the sample along with the occuring errors basing upon the formulas in the sections 2.9 and 2.10.

- Qa, dQa:  $\alpha$ -equivalent dose and its standard deviation
- Qb, dQb:  $\beta$ -equivalent dose and its standard deviation
- Intercept, dIntercept: Intercept
- aEfficiency, daEfficiency:  $\alpha$ -efficiency and its standard deviation
- AThorium:  $\alpha$ -counting rate of the thorium decay series
- AUran:  $\alpha$ -counting rate of the uranium decay series
- aCountrate, Pairs rate:  $\alpha$ -counting rate and pairs rate
- W: saturation weight increase

- F, dF: saturation fraction and its deviation
- bAttenuation:  $\beta$ -attenuation
- m: weight of  $K_2O$  in the sample in %
- DgIn: internal  $\gamma$ -dose rate
- DgExt, dDgExt: external  $\gamma$ -dose rate and its deviation
- Da, Db, Dg:  $\alpha$ -,  $\beta$ -,  $\gamma$ -dose rates
- DbThu, DbKRb:  $\beta$ -dose rates caused by thorium, uranium and potassium, rubidium
- DgIntThU, DgIntK:  $\gamma$ -dose rates caused by thorium, uranium and potassium
- Dk: cosmic dose rate
- Dtot: total dose rate
- p: self-dose percentage
- Ws: saturation weight increase of soil
- fa, fb, fg, etc: the contribution each individual dose rate adds to the annual dose rate as shown in equation (2.10)
- sig1-6: standard deviations as in section 2.10

The parameters can be saved using procedure *ButtonAgeParametersSaveClick* shown in Lst. 2 and loaded using procedure *ButtonAgeParametersLoadClick* shown in Lst. 3.

An example of the printout can be found in appendix A. Sample “PBP2” was used as base.

### Alpha-Counting Rate Unit

This dialog (Fig. 3.15) allows the calculation of the  $\alpha$ -counting rate, the pairs rate and the activities of  $^{232}\text{Th}$  and natural uranium along with their proportions of weights in ppm. Each parameter set can be saved in a text file for further utilization.



```

1 procedure TFormAge.ButtonAgeParametersSaveClick(Sender: TObject);
2 VAR DataFile : TextFile;
3 VAR Measurement : String;
4 begin
5     if SaveDialog.Execute then
6         BEGIN
7             if RadioButtonFineGrain.Checked then Measurement := '1';
8             else Measurement := '0';
9             TRY
10                AssignFile (DataFile , SaveDialog.FileName);
11                Rewrite (DataFile);
12                Writeln (DataFile
13                    EditTitle.Text+';' +
14                    EditQa.Text+';' + EditdQa.Text+';' +
15                    // ... rest of parameters
16                    LabelAge.Caption+';' + LabeldAge.Caption+';'
17                    + LabelDate.Caption+';' + LabelC.Caption+';');
18            EXCEPT
19                if BitBtnGerman.Enabled then ShowMessage ('Error Saving File!')
20                else ShowMessage ('Fehler beim Speichern der Datei!');
21            END;
22            CloseFile (DataFile);
23        END;
24    end;

```

Listing 2: Procedure *ButtonAgeParametersSaveClick* for saving parameters

```

1 procedure TFormAge.ButtonAgeParametersLoadClick(Sender: TObject);
2 VAR DataFile : TextFile;
3     Line, Measurement : String;
4     OutputValues: TStringList;
5 begin
6     OutputValues:=TStringList.Create;
7     if OpenFileDialog.Execute then
8         BEGIN
9             TRY
10                AssignFile (DataFile , OpenFileDialog.FileName);
11                Reset (DataFile);
12                WHILE NOT EOF(DataFile) DO
13                    BEGIN
14                        Readln (DataFile , Line);
15                        ExtractStrings([';','], [], String2PChar(Line), OutputValues);
16                        EditTitle.Text := OutputValues[0];
17                        // ... rest of parameters
18                        LabelC.Caption := OutputValues[44];
19                        OutputValues.Free;
20                    END;
21            EXCEPT
22                if BitBtnGerman.Enabled then ShowMessage ('Error Reading File!')
23                else ShowMessage ('Fehler beim Lesen der Datei!');
24            END;
25            CloseFile (DataFile);
26        END;
27    end;

```

Listing 3: Procedure *ButtonAgeParametersLoadClick* for loading parameters

Alpha-Counting Rate

Background (42) [Counts/ks]: 0.149 Calculate Background

Start Date: Day: 20, Month: 10, Year: 2009, Hour: 10, Minute: 47

End Date: Day: 27, Month: 10, Year: 2009, Hour: 9, Minute: 24

Difference: Minutes: 9997  
6 Days 22 Hours 37 Minutes

Countrates (Ø 42 mm)  
Total [Counts/ks]: 11,616 +/- 0.133  
Pairs [Counts/ks]: 0.257 +/- 0.019

Activities:  
Th-232 [Bq/kg]: 53,561  
nat. U [Bq/kg]: 38,091

ppm weight  
Th-232 [ppm]: 13,128 +/- 0.968  
nat. U [ppm]: 2.93 +/- 0.298

End Alpha-Counts (44): 7745  
Start Alpha-Counts (44): 0  
End Pairs-Counts (44): 203  
Start Pairs-Counts (44): 0

OK Cancel Load Save Help

Figure 3.15: Alpha-Counting Rate dialog; sample PBP2

#### Parameters:

- **Background (42) [Counts/ks]:** background value occurring during the  $\alpha$ -counting process while measuring only the scintillation film (42 mm Ø) without the sample powder, can be calculated by pressing the “Calculate Background” button as shown further below in section 3.3.3
- **Start Date:** date and time when the  $\alpha$ -counting measurement starts
- **End Date:** date and time when the  $\alpha$ -counting measurement ends
- **Start and End Alpha-Counts:**  $\alpha$ -counter reading at the beginning and at the end of the measurement
- **Start and End Pairs-Counts:** pairs count reading at the beginning and the end of the measurement when an  $\alpha$ -counter with pairs detection has been used
- **Difference:** time between the beginning and the end of the  $\alpha$ -counting measurement
- **Countrates (Ø 42 mm) [Counts/ks]:** counted  $\alpha$ -particles and coincidence pairs per ks

- **Activities [Bq/kg]:** activities of the thorium- and uranium-series as in equations (3.1), (3.2)
- **ppm weight [ppm]:** proportions of weight for thorium and uranium in ppm

#### Commands:

- **OK:** initializes all calculations and allows the return to the Age Calculation dialog with transferring the data
- **Cancel:** allows the return to the Age Calculation dialog without transferring the data
- **Load:** the currently shown parameter set along with all calculated values can be loaded from a text file
- **Save:** the currently shown parameter set along with all calculated values can be saved to a text file
- **Help:** currently not available

#### Programming:

The parameters are at first read in and afterwards the calculations of the  $\alpha$ -counting rate, the pairs rate, the activities and the proportions of weight in ppm take place in procedure *ButtonaCCalculateClick* as shown in Lst. 4.

- Background: background value in counts/ks
- NettoCounts: background subtracted from the total measured counts
- TotalCounts, dTotalCounts: amount of counted  $\alpha$ -particles per ks and its deviation
- PairCounts, dPairCounts: amount of counted coincidence pairs per ks and its deviation
- Th, U: activities of thorium and uranium
- ppmTh, ppmU: proportions of weight of thorium and uranium in ppm

The parameters can be saved and loaded analogously as shown in procedures *ButtonAgeParametersSaveClick* and *ButtonAgeParametersLoadClick* in Lst. 2 and Lst. 3.

```

1 procedure TFormaCountrate.ButtonaCCalculateClick(
2     Sender: TObject);
3
4     //... variables are defined
5
6 begin
7
8     //... parameters are read in and the time difference is calculated
9
10    begin
11        Background:=StrToFloat(LabelBackground.Caption);
12        NettoCounts:=TotalEnd-TotalStart-
13            Background*Mins*60/1000*sqr(44)/sqr(42);
14        TotalCounts:=NettoCounts/(Mins*60)*1000*sqr(42)/sqr(44);
15        if NettoCounts > 0 then
16            begin
17                dTotalCounts:=sqrt(NettoCounts)/(Mins*60)*1000*sqr(42)/sqr(44);
18            end;
19        LabelTotalCounts.Caption:=FloatToStr(Round(1000*TotalCounts)/1000);
20        LabeldTotalCounts.Caption:=FloatToStr(Round(1000*dTotalCounts)/1000);
21        BruttoPairCounts:=(PairEnd-PairStart)/(Mins*60)*1000*sqr(42)/sqr(44);
22        PairCounts:=BruttoPairCounts-0.38*sqr(TotalCounts)/1000;
23        IF PairCounts<0 THEN PairCounts:=0;
24        dPairCounts:=sqrt(Paircounts*Mins*60/1000+sqr(44)/sqr(42))/
25            (Mins*60)*1000*sqr(42)/sqr(44);
26        LabelPairCounts.Caption:=FloatToStr(Round(1000*PairCounts)/1000);
27        LabeldPairCounts.Caption:=FloatToStr(Round(1000*dPairCounts)/1000);
28
29        Th:=PairCounts/0.0048;
30        U :=(TotalCounts-0.123*Th)/0.132;
31        LabelTh.Caption:=FloatToStr(Round(1000*Th)/1000);
32        LabelU.Caption:=FloatToStr(Round(1000*U)/1000);
33
34        ppmTh:=Th/4.08;
35        ppmU :=U/13;
36        dppmTh:=1/(4.08*0.0048)*sqrt(sqr(dPairCounts)+
37            sqr(2*0.38/1000*TotalCounts*dTotalCounts));
38        dppmU:=1/(13*0.132)*sqrt(
39            sqr(dTotalCounts+
40            2*0.123*0.38/0.0048/1000*TotalCounts*dTotalCounts)+
41            sqr(0.123/0.0048*dPairCounts));
42        LabelppmTh.Caption:=FloatToStr(Round(1000*ppmTh)/1000);
43        LabelppmU.Caption:=FloatToStr(Round(1000*ppmU)/1000);
44        LabeldppmTh.Caption:=FloatToStr(Round(1000*dppmTh)/1000);
45        LabeldppmU.Caption:=FloatToStr(Round(1000*dppmU)/1000);
46    end;
47 end;

```

Listing 4: Procedure *ButtonaCCalculateClick* manages the calculation of the  $\alpha$ -counting rate and pairs rate

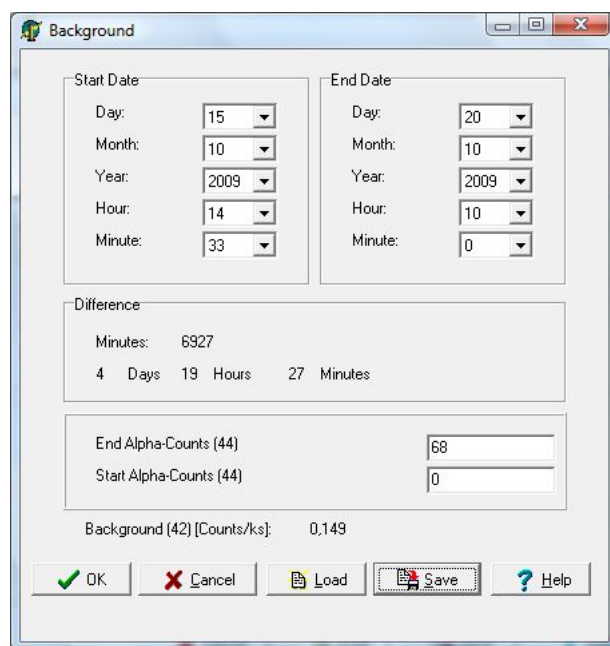


Figure 3.16: Background dialog; sample PBP2

## Background Unit

This dialog (Fig. 3.16) allows the calculation of the background value. Each parameter set can be saved in a text file for further utilization.

### Parameters:

- **Start Date:** date and time when the  $\alpha$ -counting measurement starts
- **End Date:** date and time when the  $\alpha$ -counting measurement ends
- **Difference:** time between the beginning and the end of the  $\alpha$ -counting measurement
- **Start and End Alpha-Counts:** amount of counted  $\alpha$ -particles using the  $\alpha$ -counter at the beginning and the end of the measurement of scintillation film without the sample powder
- **Background (42) [Counts/ks]:** calculated background value

### Commands:

- **OK:** initializes all calculations and allows the return to the Alpha-Counting Rate dialog with transferring the data

```

1 procedure TFormBackground.ButtonBGCalculateClick(Sender: TObject);
2
3     // ... variables are defined
4
5 begin
6
7     // ... parameters are read in and the time difference calculated
8
9     begin
10         Background := (TotalEnd - TotalStart) / (Mins * 60) * 1000 * sqr(42) / sqr(44);
11         LabelBackground.Caption := FloatToStr(Round(1000 * Background) / 1000);
12     end;
13 end;

```

Listing 5: Procedure *ButtonBGCalculateClick* manages the calculation of the background value

- **Cancel:** allows the return to the Alpha-Counting Rate dialog without transferring the data
- **Load:** the currently shown parameter set along with all calculated values can be loaded from a text file
- **Save:** the currently shown parameter set along with all calculated values can be saved to a text file
- **Help:** currently not available

### Programming:

The parameters are read in and the calculation of the background value is made in procedure *ButtonBGCalculateClick* as shown in Lst. 5.

- TotalEnd, TotalStart: amount of counted  $\alpha$ -particles at the beginning and the end of measurement
- Background: background value in counts/ks

The parameters can be saved and loaded analogously as shown in procedures *ButtonAgeParametersSaveClick* and *ButtonAgeParametersLoadClick* in Lst. 2 and Lst. 3.

### Saturation Fraction/Saturation Weight Increase Unit

This dialog (Fig. 3.17) allows the calculation of the saturation fraction and

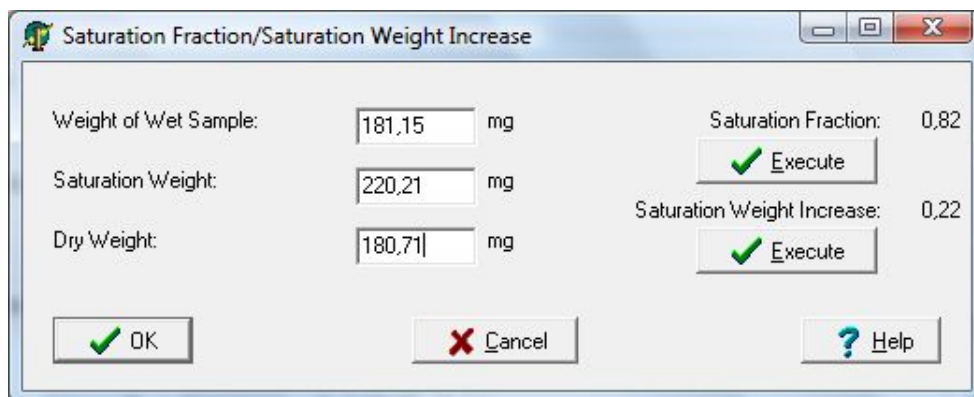


Figure 3.17: Saturation Fraction/Saturation Weight Increase dialog; sample PBP2

saturation weight by entering the needed parameters.

#### Parameters:

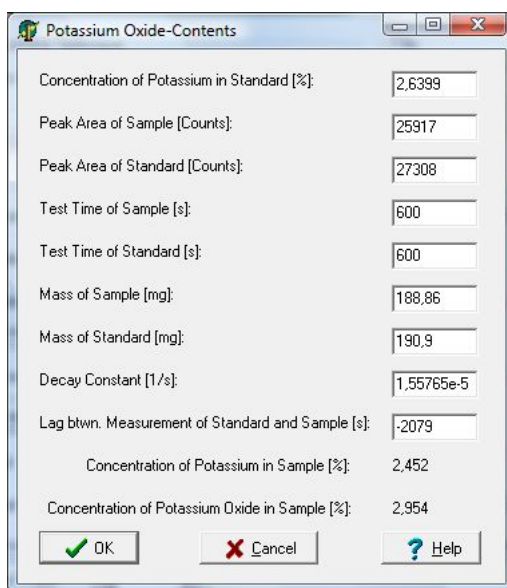
- **Weight of Wet Sample [mg]:** immediately determined weight of a fragment separated from the sample
- **Saturation Weight [mg]:** weight of a fragment stored in distilled water for a few days
- **Dry Weight [mg]:** weight of a fragment after drying it for a few days
- **Saturation Fraction:** wetness
- **Saturation Weight Increase:** increase of weight when water content is saturated

#### Commands:

- **Execute:** initializes the calculation for the saturation fraction and the saturation weight increase respectively
- **OK:** allows the return to the Age Calculation dialog with transferring the calculated data
- **Cancel:** allows the return to the Alpha-Counting Rate dialog without transferring the data
- **Help:** currently not available

### Programming:

The parameters are read in and the calculation of the saturation fraction, equation (2.21), and of the saturation weight increase, equation (2.20), is performed.



Parameter	Value
Concentration of Potassium in Standard [%]	2.6399
Peak Area of Sample [Counts]	25917
Peak Area of Standard [Counts]	27308
Test Time of Sample [s]	600
Test Time of Standard [s]	600
Mass of Sample [mg]	188.86
Mass of Standard [mg]	190.9
Decay Constant [1/s]	1.55765e-5
Lag btwn. Measurement of Standard and Sample [s]	-2079
Concentration of Potassium in Sample [%]	2.452
Concentration of Potassium Oxide in Sample [%]	2.954

Figure 3.18: Potassium Oxide-Contents dialog; standard SO-1 with sample PBP2

### Potassium Oxide-Contents Unit

This dialog (Fig. 3.18) allows the calculation of the  $K_2O$ -concentration within the sample. Values are received as explained in section 3.1.3. On opening the dialog some default values are displayed.

#### Parameters:

- **Concentration of Potassium in Standard [%]:** known percentage of potassium in a standard material
- **Peak Area of Sample [Counts]:** counts of the sample occurring during  $\gamma$ -spectroscopy
- **Peak Area of Standard [Counts]:** counts of the standard occurring during  $\gamma$ -spectroscopy
- **Test Time of Sample [s]:** time of measurement of the sample in s



- **Test Time of Standard [s]:** time of measurement of the standard in s
- **Mass of Sample [mg]:** mass of the sample in mg
- **Mass of Standard [mg]:** mass of the standard in mg
- **Decay Constant [1/s]:** decay constant for  $^{42}\text{K}$ :  $1.55764811 \cdot 10^{-5}$
- **Lag btwn. Measurement of Standard and Sample:** time elapsed between starting measurement of standard and sample in s; it has to be entered with a minus when the sample is measured before the standard
- **Concentration of Potassium in Sample [%]:** calculated potassium concentration in the sample in percent
- **Concentration of Potassium Oxide in Sample [%]:** calculated potassium oxide-concentration in percent

By pressing “OK” the calculation of potassium and potassium oxide-concentrations within the sample is initialized and the dialog is closed with transferring the data to the Age Calculation dialog.

#### **Programming:**

The parameters are read in and the calculation of the potassium and potassium oxide-concentrations is made in procedure *ButtonK2OCalculateClick* as shown in Lst. 6.

- CSample: concentration of potassium within the sample in percent
- CK2OSample: concentration of potassium oxide within the sample in percent

#### **External $\gamma$ -Dose Rate Unit**

This dialog (Fig. 3.19) allows the calculation of the corrected external  $\gamma$ -dose rate after measurement at the excavation site.

#### **Parameters:**

- **Measured  $\gamma$ -Dose Rate [mGy/a]:**  $\gamma$ -dose rate measured at the excavation site

```

1 procedure TFormK2O.ButtonK2OCalculateClick(Sender: TObject);
2
3     //... variables are defined
4
5 begin
6
7     Error := False;
8
9     //... parameters are read in
10
11 if Error then begin
12     if FormAge.BitBtnGerman.Enabled then Showmessage('Check Entries!')
13     else Showmessage('Eingaben überprüfen!')
14     end
15 else begin
16     CSample := CStand*(NSample*exp(Lambda*TD)*TStand*mStand)/
17             (NStand*TSample*mSample);
18     CK2OSample := CSample*1.205;
19     LabelCSample.Caption := FloatToStr(Round(1000*CSample)/1000);
20     LabelCK2OSample.Caption := FloatToStr(Round(1000*CK2OSample)/1000);
21 end;
22
23 end;

```

Listing 6: Procedure *ButtonK2OCalculateClick* manages the calculation of the potassium and potassium oxide-concentrations within the sample

Parameter	Value
Measured $\gamma$ - Dose-Rate ( $\dot{D}_{\gamma \text{ TLD}}$ ) [mGy/a]	0,532
Saturation Weight Increase of Soil:	0,2
Wetness of Soil:	0
Saturation Fraction:	0,8
Cosmic Dose-Rate ( $\dot{D}_c$ ) [mGy/a]	0,281
External $\gamma$ - Dose-Rate ( $\dot{D}_{\gamma \text{ ext}}$ ) [mGy/a]	0,169

Buttons: OK, Cancel, Help

Figure 3.19: External  $\gamma$ -Dose Rate; sample PBP2

```

1 procedure TFormBackground.ButtonBGCalculateClick(Sender: TObject);
2
3     // ... variables are defined
4
5 begin
6
7     // ... parameters are read in and the time difference calculated
8
9     begin
10        Background := (TotalEnd - TotalStart) / (Mins * 60) * 1000 * sqrt(42) / sqrt(44);
11        LabelBackground.Caption := FloatToStr(Round(1000 * Background) / 1000);
12    end;
13 end;

```

Listing 7: Procedure *ButtonDgExtCalculateClick* manages the calculation of the corrected  $\gamma$ -dose rate

- **Saturation Weight Increase of Soil:** increase of weight of soil when water content is saturated, value is adopted from the Age Calculation dialog if defined there
- **Wetness of Soil:** wetness of soil due to environmental influences
- **Saturation Fraction:** wetness of sample, value is adopted from the Age Calculation dialog if defined there
- **Cosmic Dose Rate [mGy/a]:** annual cosmic dose rate, value is adopted from the Age Calculation dialog if defined there
- **External  $\gamma$ -Dose Rate [mGy/a]:** corrected annual  $\gamma$ -Dose Rate, equation (2.35)

By pressing “OK” the calculation is initialized and the dialog is closed with transferring the data to the Age Calculation dialog.

### Programming:

The parameters are read in and the calculation of the corrected  $\gamma$ -dose rate is made in procedure *ButtonDgExtCalculateClick* as shown in Lst. 7.

- DgExt: corrected  $\gamma$ -dose rate
- DgTLD: measured  $\gamma$ -dose rate
- Dk: cosmic dose rate
- F: saturation fraction

- Ws: saturation weight increase of soil
- Fs: wetness of soil

**Cosmic Dose-Rate**

**Excavation Site:** Petronell-Carnuntum

**Geographical Position:**  
 (North Latitude/East Longitude (positive),  
 South Latitude/West Longitude (negative)):

Latitude: 48 ° 7 '

Longitude: 16 ° 51 '

Lambda: 11,26

F:

J:

H [km]:

Sea Level of Excavation Site [m]:

Cosmic Dose-Rate ( $\dot{D}_e$ ) [mGy/a]: 0,176

Figure 3.20: Cosmic Dose Rate dialog; sample PBP2

### Cosmic Dose Rate Unit

This dialog (Fig. 3.20) allows the calculation of the cosmic dose rate. The name of the excavation site and geographical position can be entered, which will then be shown in the printout.

#### Parameters:

- **Latitude:** latitude of the excavation site in degrees and minutes, whereas the north latitude is entered without an algebraic sign and the south latitude is entered with a minus in front of the number
- **Longitude:** longitude of the excavation site in degrees and minutes, whereas the east longitude is entered without an algebraic sign and the west longitude is entered with a minus in front of the number
- **Lambda:** geomagnetic latitude, equation (3.10)
- **F, J, H [km]:** constants, integrated in the software; readable in Fig. 3.4

```

1 procedure TFormDk.ButtonLCalculateClick(Sender: TObject);
2 VAR Lat, Long, lambda, cosLat, CosPhi, SinLat : Real;
3 VAR curve: TCurve;
4     triple: TCurveTriple;
5 begin
6     Lat := StrToFloat(EditLongDegree.Text)+(StrToFloat(EditLongMin.Text)/60);
7     Long := StrToFloat(EditLatDegree.Text)+StrToFloat(EditLatMin.Text)/60;
8     cosLat := cos(DegToRad(Lat));
9     sinLat := sin(DegToRad(Lat));
10    cosphi := cos(DegToRad(Long-291));
11    lambda := RadToDeg( arcsin(0.203*cosLat*cosphi+0.979*sinLat));
12    LabelLambda.Caption := FloatToStr(Round(100*lambda)/100);
13    curve := TCurve.Create;
14    triple := curve.GetTriple(lambda);
15
16    EditF.Text := FloatToStr(triple.FWert);
17    EditJ.Text := FloatToStr(triple.JWert);
18    EditH.Text := FloatToStr(triple.HWert);
19    curve.Free;
20 end;

```

Listing 8: Procedure *ButtonLCalculateClick* manages the calculation of the geomagnetic latitude

- **Sea Level of Excavation Site [m]:** sea level of the excavation site of the sample in meters
- **Cosmic Dose Rate [mGy/a]:** calculated annual cosmic dose rate, equation (3.9)

#### Commands:

- **Lambda:** initializes the calculation of the geomagnetic latitude
- **OK:** initializes the calculation of the cosmic dose rate and allows the return to the Age Calculation dialog with transferring the data
- **Execute:** initializes the calculation of the cosmic dose rate
- **Cancel:** allows the return to the Age Calculation dialog without transferring the data
- **Help:** currently not available

#### Programming:

The parameters of the geomagnetic latitude are read in and the calculation is made in procedure *ButtonLCalculateClick* as shown in Lst. 8. The values of the constants J, F and H are displayed in the dialog.

```

1 procedure TFormDk.ButtonDkCalculateClick(Sender: TObject);
2 var Dk, K, F, J, SeaLevel, H : Real;
3     Error : boolean;
4 begin
5     Error := False;
6     K := 0.185;
7
8     // ... parameters are read in
9
10    if Error then begin
11        if FormAge.BitBtnGerman.Enabled then Showmessage('Check Entries!')
12        else Showmessage('Eingaben überprüfen!')
13    end
14    else
15        if H < 0 then
16            begin
17                Dk := K*(F+J*exp(SeaLevel/(H*1000)));
18                LabelDk.Caption := FloatToStr(Round(1000*Dk)/1000);
19            end;
20    end;

```

Listing 9: Procedure *ButtonDkCalculateClick* manages the calculation of the cosmic dose rate

- cosLat: cosine of the geographic latitude
- sinLat: sine of the geographic latitude
- cosphi: cosine of the geographic longitude
- lanbda: calculated geomagnetic latitude

The parameters of the cosmic dose rate are read in and the calculation is made in procedure *ButtonDkCalculateClick* as shown in Lst. 9.

- K: constant; 0.185 mGy/a
- Dk: calculated cosmic dose rate

## Error Caused by Stony Surroundings Unit

This dialog (Fig. 3.21) allows the calculation of the error caused by stony surroundings.

### Parameters:

- **Total Dose Rate [mGy/a]:** total dose rate, value is adopted from the Age Calculation dialog if defined there

Figure 3.21: Error Caused by Stony Surroundings dialog; sample PBP2

```

1  procedure TFormErrorStoneContent.ButtonSigma3CalculateClick(Sender: TObject);
2  var Sigma3, DTotal, Dg, Dg1, Dg2, r : Real;
3      Error : Boolean;
4  begin
5      Error := False;
6
7      // ... parameters are read in
8
9      if Error then begin
10         if FormAge.BitBtnGerman.Enabled then Showmessage('Check Entries!')
11         else Showmessage('Eingaben überprüfen!')
12         end
13     else begin
14         if (DTotal > 0) and (Dg > 0) then
15             begin
16                 Sigma3 := 100*r*Dg/DTotal*((Dg1-Dg2)/Dg);
17                 LabelSigma3.Caption := FloatToStr(Round(100*Sigma3)/100)
18             end
19         else begin
20             LabelSigma3.Caption := '0'
21         end;
22     end;
23 end;

```

Listing 10: Procedure *ButtonSigma3CalculateClick* manages the calculation of error caused by stony surroundings

- **$\gamma$ -Dose Rate [mGy/a]:**  $\gamma$ -dose rate, value is adopted from the Age Calculation dialog if defined there
- **$\gamma$ -Dose Rate of Soil Surrounding Sample [mGy/a]:** measured  $\gamma$ -dose rate of the soil surrounding the sample
- **$\gamma$ -Dose Rate of Stones [mGy/a]:** measured  $\gamma$ -dose rate of stones surrounding the sample
- **Actual Weight Component of Stones in Surroundings of Sample**
- **Sigma [%]:** calculated error caused by stony surroundings, equation (2.41)

By pressing “OK” the calculation of the error is initialized and the dialog is closed with transferring the data to the Age Calculation dialog.

#### **Programming:**

The parameters are read in and the calculation of the error caused by stony surroundings is made in procedure *ButtonSigma3CalculateClick* as shown in Lst. 10.

- sigma3: calculated error
- DTotal: total dose rate
- Dg:  $\gamma$ -dose rate
- D1:  $\gamma$ -dose rate of soil surrounding sample
- D2:  $\gamma$ -dose rate of stones
- r: actual weight component of stones in surroundings of the sample



## 4 Results of Thermoluminescence Age Determination

For all samples the sample powder was obtained by drilling. Afterwards fractionation and sedimentation were carried out as explained in the sections 3.2.2-3.2.5. The samples were measured according to section 3.3. For checking the software the first task was to evaluate the age of a clay brick from Alkoven whose age had been determined several times and after that a sample from Petronell-Carnuntum was measured. The revised software for the dating process was compared to the original one to confirm its equivalence.

### 4.1 Sample from Alkoven, “PBP1”



Figure 4.1: Sample “PBP1”; coated aluminium discs

Figures 4.2-4.15 show the  $\alpha$ - and  $\beta$ -irradiated glow-curves, the second-glow-curves, the plateau test, the regression lines and the determined age of the sample “PBP1” for both the original and revised software. Depending on the used software additionally irradiated glow-curve names are displayed for example as NB1 or N $\beta$ 1. The notation further on uses Greek letters.

In Fig. 4.2 and Fig. 4.3 two natural glow-curves (N00) are displayed along with seven  $\alpha$ -irradiated glow-curves (N $\alpha$ 1  $\cong$  15.62 Gy, N $\alpha$ 2  $\cong$  31.24 Gy, N $\alpha$ 3  $\cong$  46.86 Gy, N $\alpha$ 4  $\cong$  62.48 Gy).

Figures 4.4 and 4.5 show two natural glow-curves (N00) and seven  $\beta$ -irradiated glow-curves (N $\beta$ 1  $\cong$  1.98 Gy, N $\beta$ 2  $\cong$  3.96 Gy, N $\beta$ 3  $\cong$  5.93 Gy, N $\beta$ 4  $\cong$  7.91 Gy).

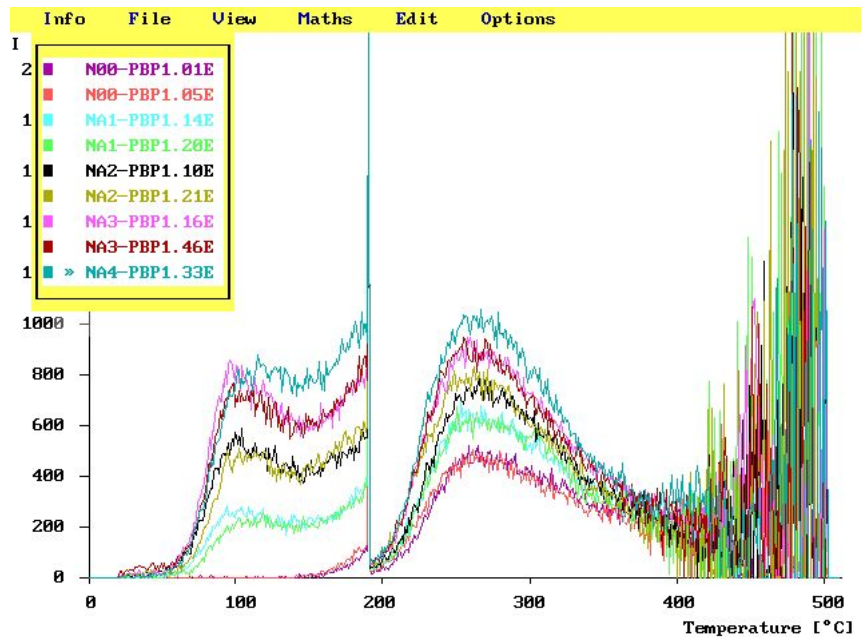


Figure 4.2: Natural and  $\alpha$ -irradiated glow-curves of sample “PBP1” - original software

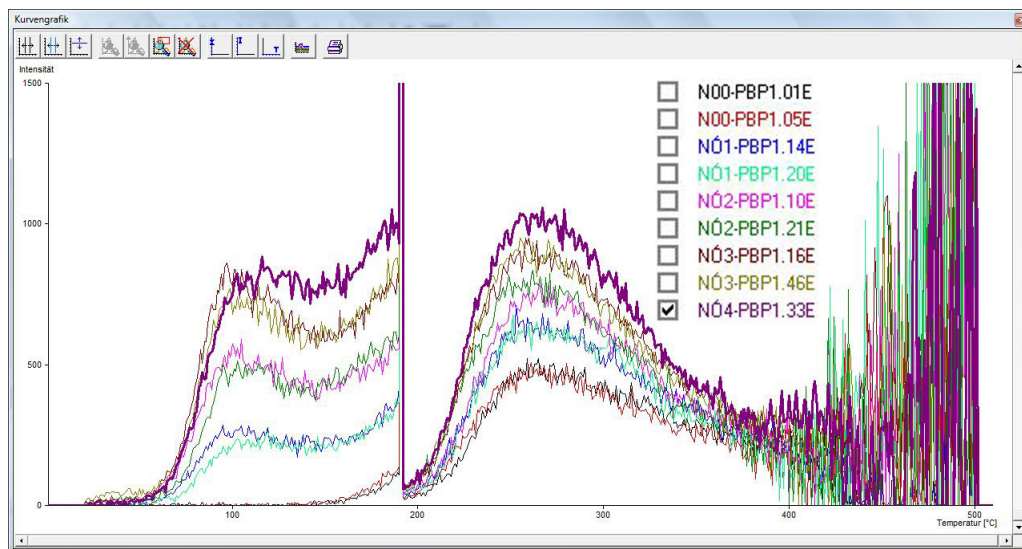


Figure 4.3: Natural and  $\alpha$ -irradiated glow-curves of sample “PBP1” - revised software

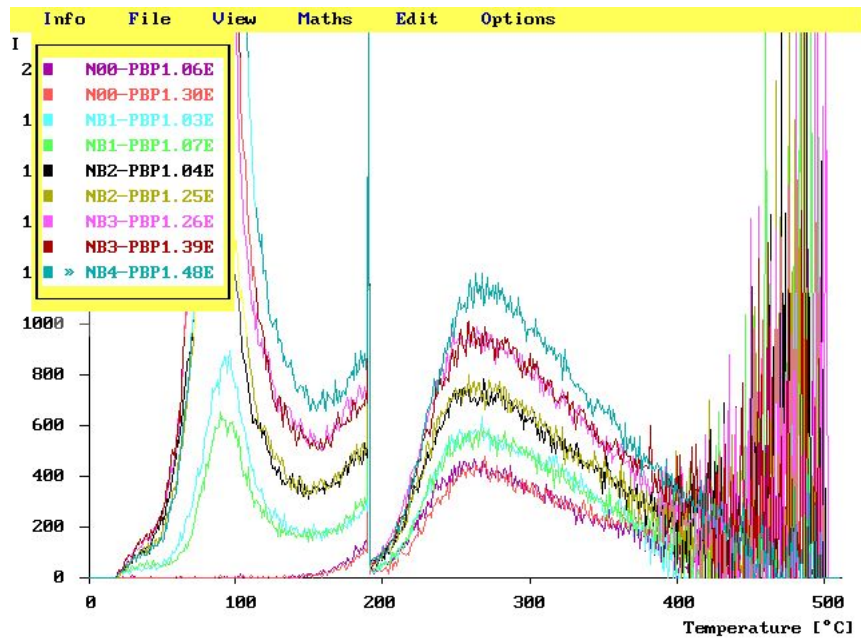


Figure 4.4: Natural and  $\beta$ -irradiated glow-curves of sample “PBP1” - original software

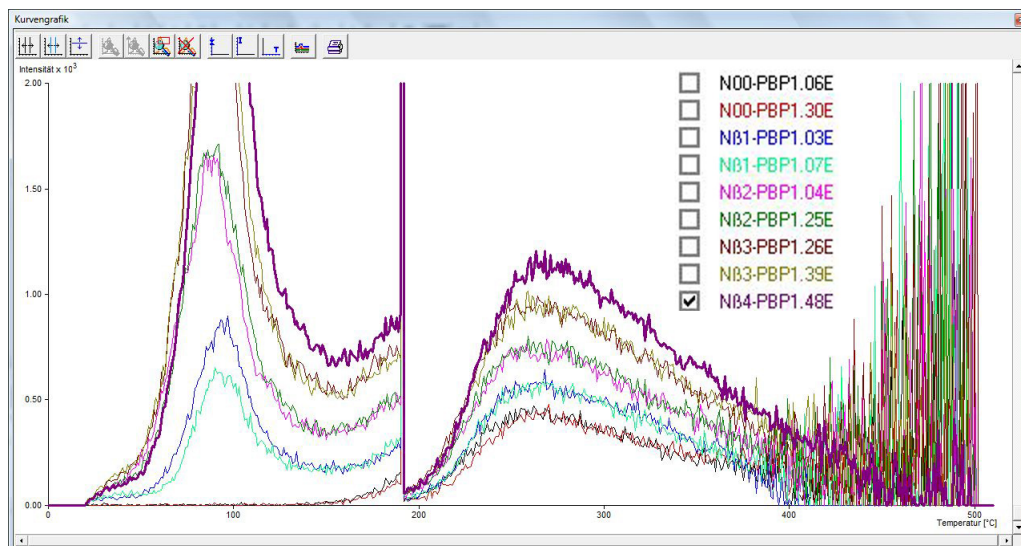


Figure 4.5: Natural and  $\beta$ -irradiated glow-curves of sample “PBP1” - revised software

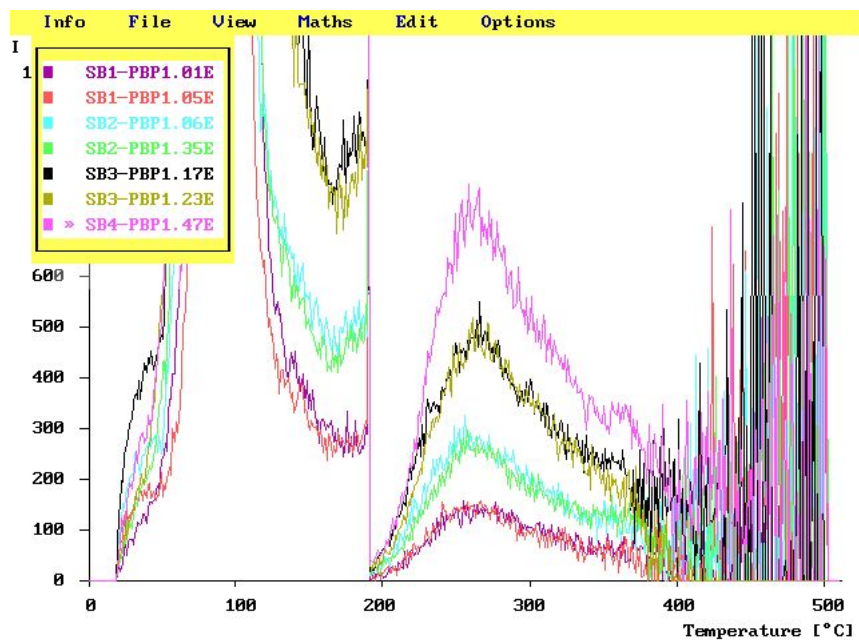


Figure 4.6: Second-glow-curves of sample “PBP1” - original software

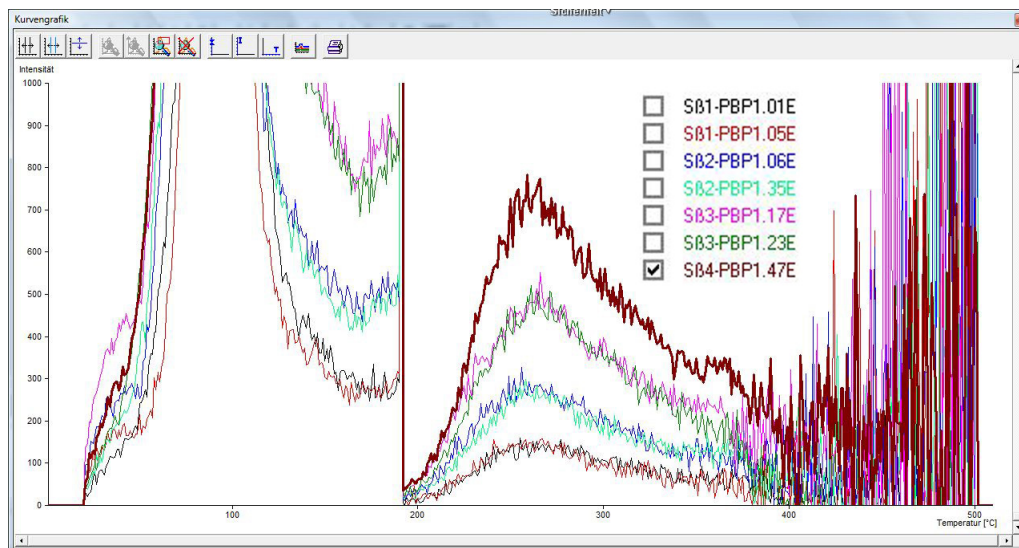


Figure 4.7: Second-glow-curves of sample “PBP1” - revised software

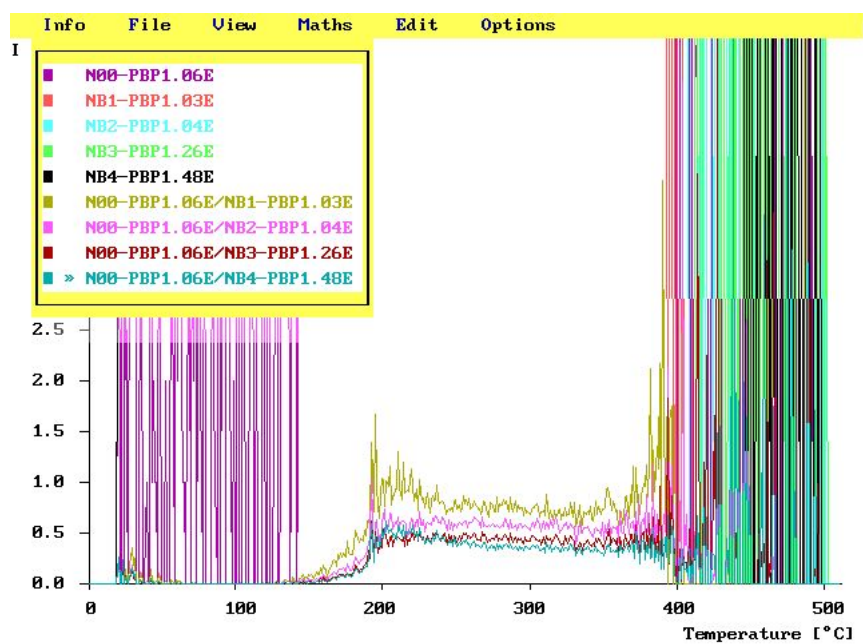


Figure 4.8: Plateau test of sample “PBP1” - original software

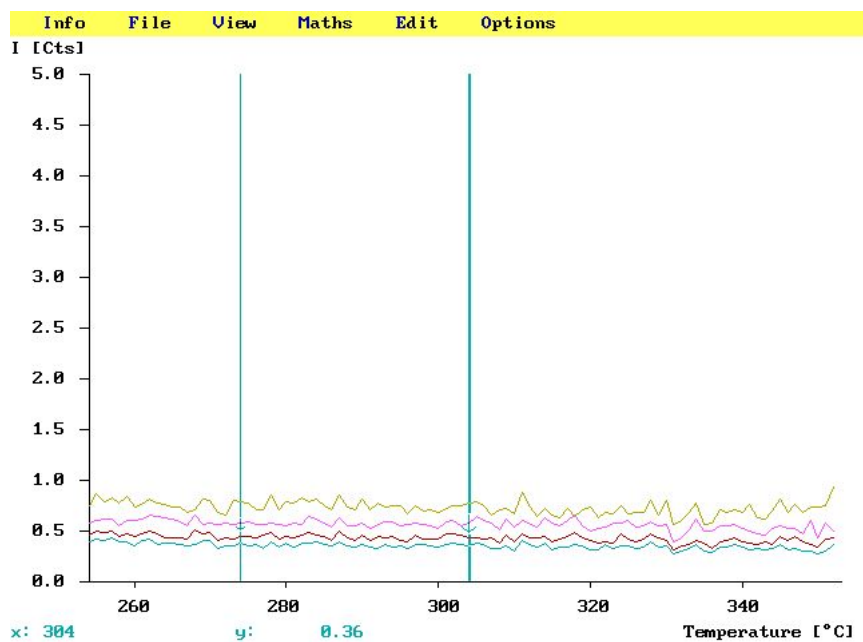


Figure 4.9: Plateau test with zoomed integration interval (276-304 °C) of sample “PBP1” - original software



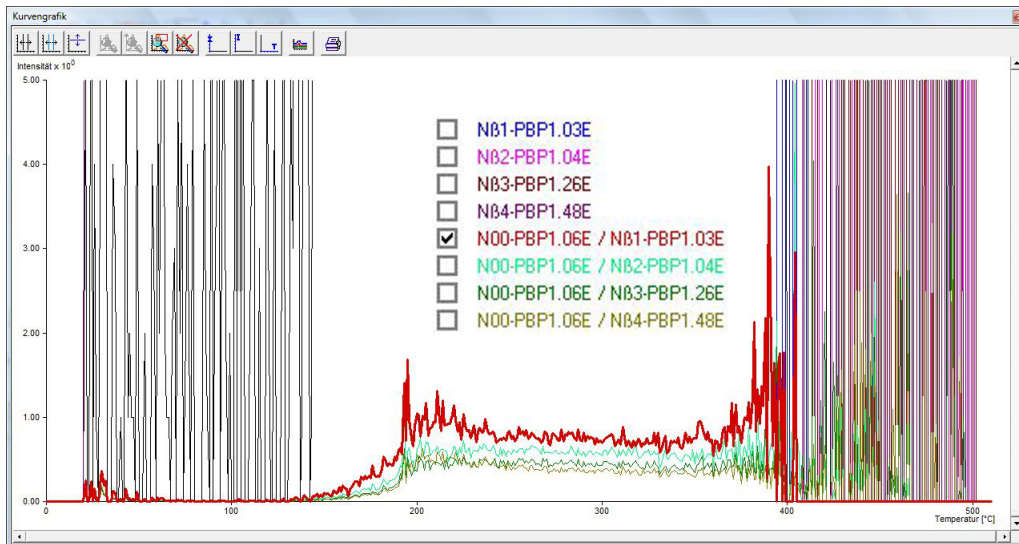


Figure 4.10: Plateau of sample “PBP1” - revised software

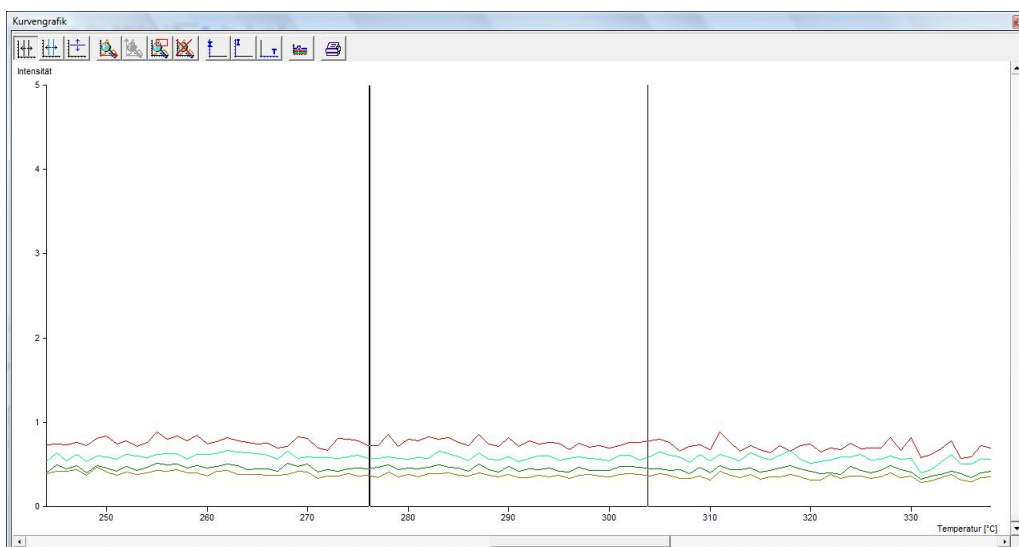


Figure 4.11: Plateau test with zoomed integration interval (276-304 °C) of sample “PBP1” - revised software

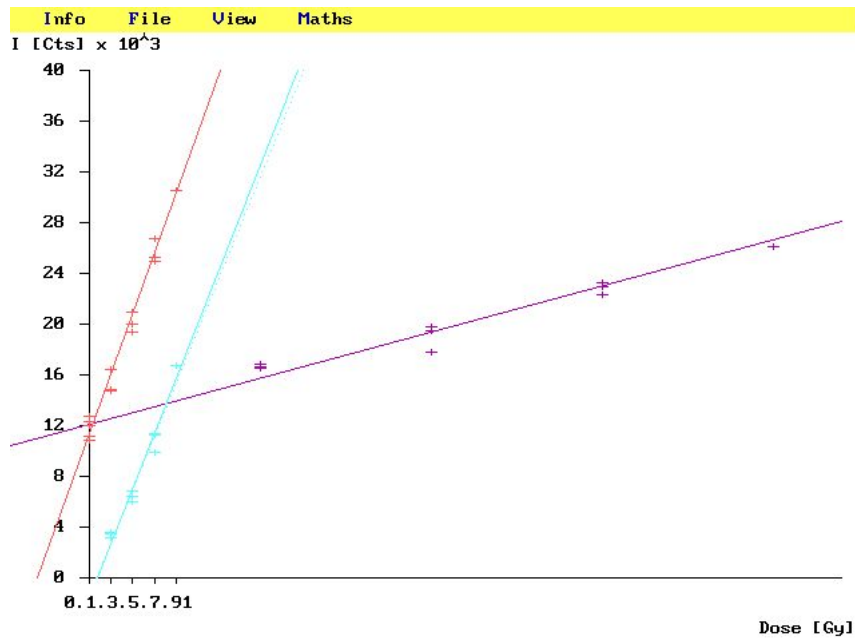


Figure 4.12: Regression lines of sample “PBP1” - original software

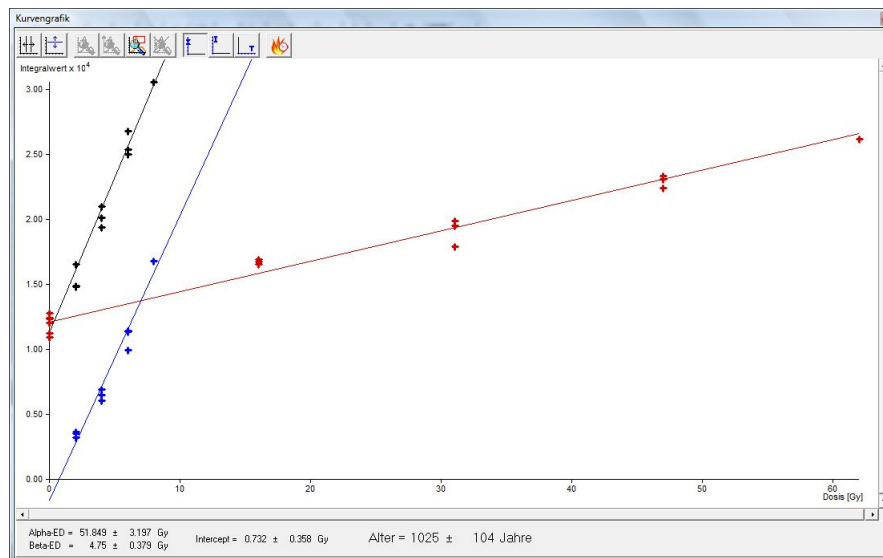


Figure 4.13: Regression lines of sample “PBP1” - revised software

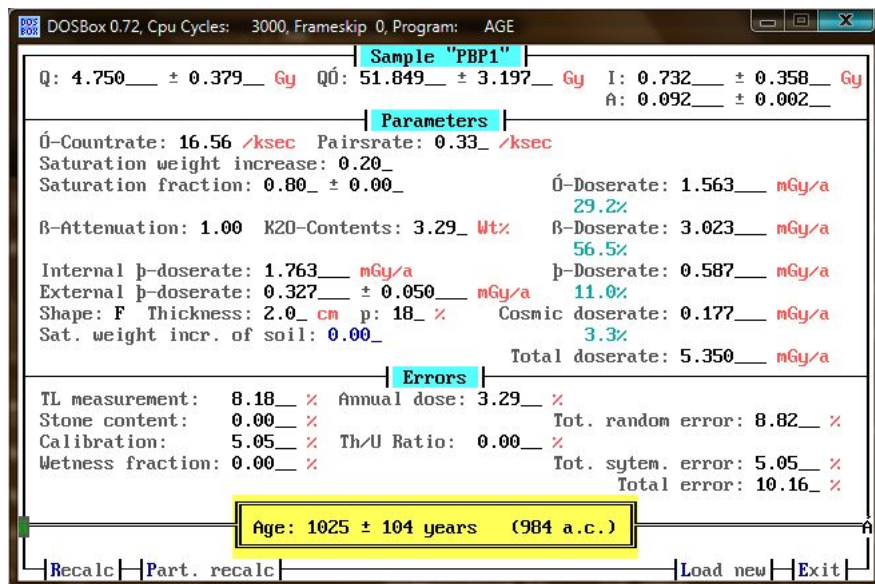


Figure 4.14: Age Calculation of sample "PBP1" - original software

**Age Calculation**

Measurement Technique: ☒ Fine Grain Technique ☐ Inclusion Technique

Title: Sample "PBP1"

Date of Measurement: 07.10.2009

Q<sub>α</sub>: 51.849 ± 3.197 Gy Q<sub>β</sub>: 4.75 ± 0.379 Gy I: 0.732 ± 0.358 Gy A: 0.092 ± 0.002

α - Counting Rate: 16.561 Counts/ks Pairs Rate: 0.33 Counts/ks

Saturation Weight Increase: 0.2

Saturation Fraction: 0.8 ± 0 Effective α - Dose-Rate (D<sub>α</sub>): 1.563 mGy/a 29.21 %

K<sub>2</sub>O-Contents: 3.29 Wt% β - Attenuation: 1 β - Dose-Rate (D<sub>β</sub>): 3.023 mGy/a 56.5 %

Internal γ - Dose-Rate (D<sub>γ int</sub>): 1.763 mGy/a γ - Dose-Rate (D<sub>γ</sub>): 0.587 mGy/a 10.97 %

External γ - Dose-Rate (D<sub>γ ext</sub>): 0.327 ± 0.050 mGy/a Cosmic Dose-Rate (D<sub>c</sub>): 0.177 mGy/a 3.31 %

Sample Shape: flat

Sample Thickness: 2 cm

p: 18.13 %

Saturation Weight Increase of Soil: 0

Total Dose-Rate (D): 5.35 mGy/a

TL Measurement: 8.18 %  
Annual Dose: 3.29 %  
Stone Content: 0 %  
  
Total Random Error: 8.82 %  
Calibration: 5.05 %  
Th/U-Ratio: 0 %  
Wetness: 0 %  
Total Systematic Error: 5.05 %  
Total Error: 10.16 %

Age  
**Age 1025 ± 104 Years**  
(984 a.c.)

Figure 4.15: Age Calculation of sample "PBP1" - revised software



In Fig. 4.6 and Fig. 4.7 the second-glow-curves are displayed.

Figures 4.8-4.11 show the plateau test of a natural glow-curve and four different  $\beta$ -irradiated glow-curves. Furthermore the area is expanded to determine a suitable integration interval. In this case the interval from 276 °C to 304 °C was chosen.

In Figures 4.12 and 4.13 the regression lines can be seen. (Fig. 4.12:  $\alpha$ -regressionline: violet,  $\beta$ -regression line: red, second-glow-curve-regression line: blue; Fig. 4.13:  $\alpha$ -regressionline: red,  $\beta$ -regression line: black, second-glow-curve-regression line: blue) The parallelism of the  $\beta$ - and the second-glow-regression line is definitely obvious.

Fig. 4.14 and Fig. 4.15 show the calculation of the age, the result and its error. As the parameters needed for the determination of the age of the brick had been determined several times and the weight of the wet sample might be affected by the long storage, the values of the saturation fraction and the saturation weight increase were adopted. The  $\alpha$ -counting rate, the pairs rate and the potassium oxide concentration were measured and together with the cosmic dose rate calculated in the age calculation program module as described in section 3.3.3. The external  $\gamma$ -dose rate was taken from the Austrian Radiation Map (Tschirf et al., 1970) [23].

**Determined parameters (see section 3.1):**

- $\alpha$ -counting rate [Counts/ks]: 16.561
- Pairs rate [Counts/ks]: 0.33
- $K_2O$ -contents [%]: 3.29; was determined by measuring the sample along with two standard materials, the average value was taken
- External  $\gamma$ -dose rate [mGy/a]: 0.327
- Cosmic dose rate [mGy/a]: 0.177

## 4.2 Sample from Petronell-Carnuntum, “PBP2”



Figure 4.16: Sample “PBP2”; coated aluminium discs

Figures 4.18-4.23 show the  $\alpha$ - and  $\beta$ -irradiated glow-curves, the second-glow-curves, the plateau test, the regression lines and the determined age of the sample “PBP2”.

In Fig. 4.17 two natural glow-curves (N00) are displayed along with seven  $\alpha$ -irradiated glow-curves ( $N_{\alpha 1} \cong 15.62$  Gy,  $N_{\alpha 2} \cong 31.24$  Gy,  $N_{\alpha 3} \cong 46.86$  Gy,  $N_{\alpha 4} \cong 62.48$  Gy).

Figure 4.18 shows two natural glow-curves (N00) and seven  $\beta$ -irradiated glow-curves ( $N_{\beta 1} \cong 1.98$  Gy,  $N_{\beta 2} \cong 3.96$  Gy,  $N_{\beta 3} \cong 5.93$  Gy,  $N_{\beta 4} \cong 7.91$  Gy).

In Fig. 4.6 the second-glow-curves are displayed.

Figures 4.20 and 4.21 show the plateau test of a natural glow-curve and four different  $\beta$ -irradiated glow-curves. Furthermore, the area is magnified as to determine a suitable integration interval. In this case the interval from 270 °C to 300 °C was chosen.

In Figure 4.22 the regression lines can be seen. ( $\alpha$ -regressionline: red,  $\beta$ -regression line: black, second-glow-curve-regression line: blue) The parallelity of the  $\beta$ - and the second-glow-regression line is definitely obvious.

Fig. 4.23 shows the calculation of the age, the result and its error.

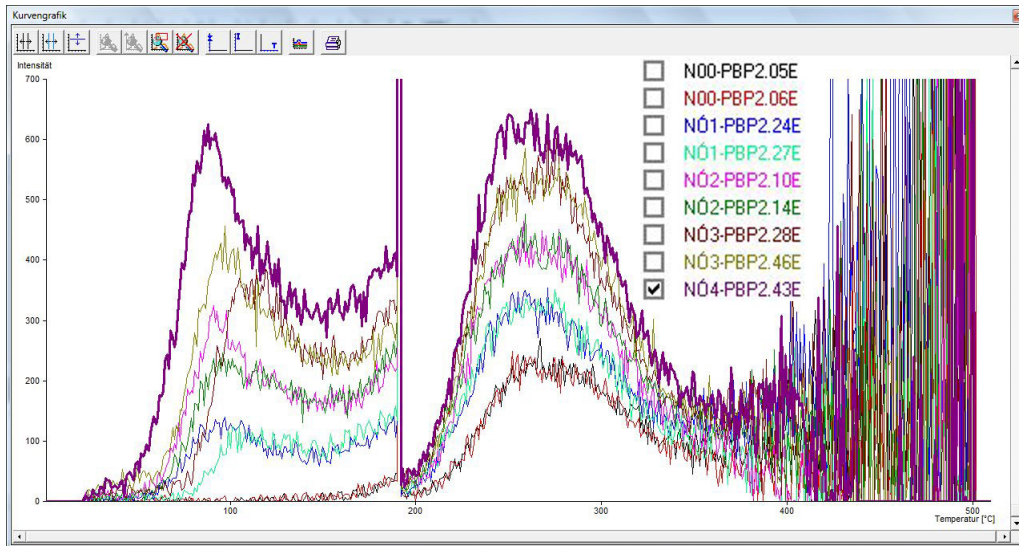


Figure 4.17: Natural and  $\alpha$ -irradiated glow-curves of sample "PBP2"

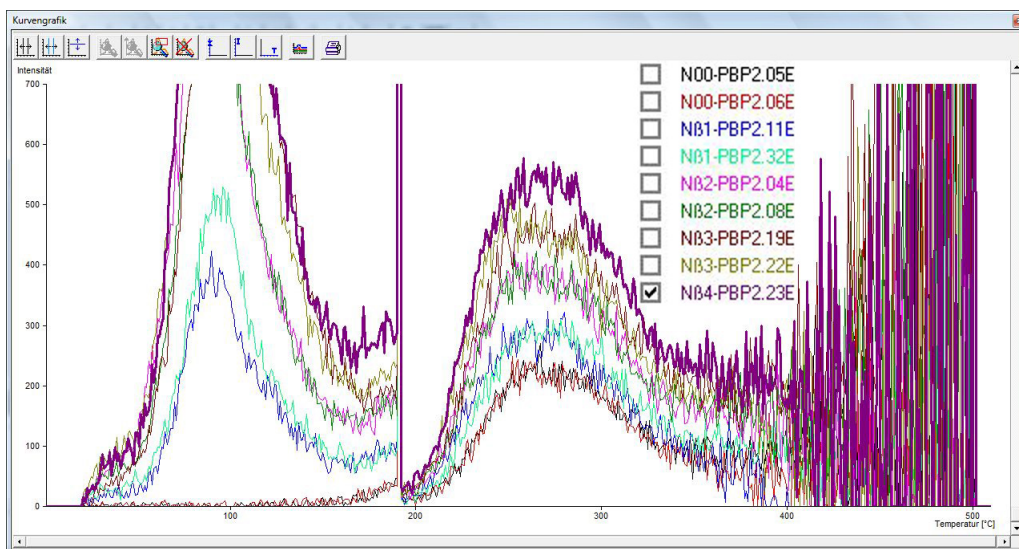


Figure 4.18: Natural and  $\beta$ -irradiated glow-curves of sample "PBP2"

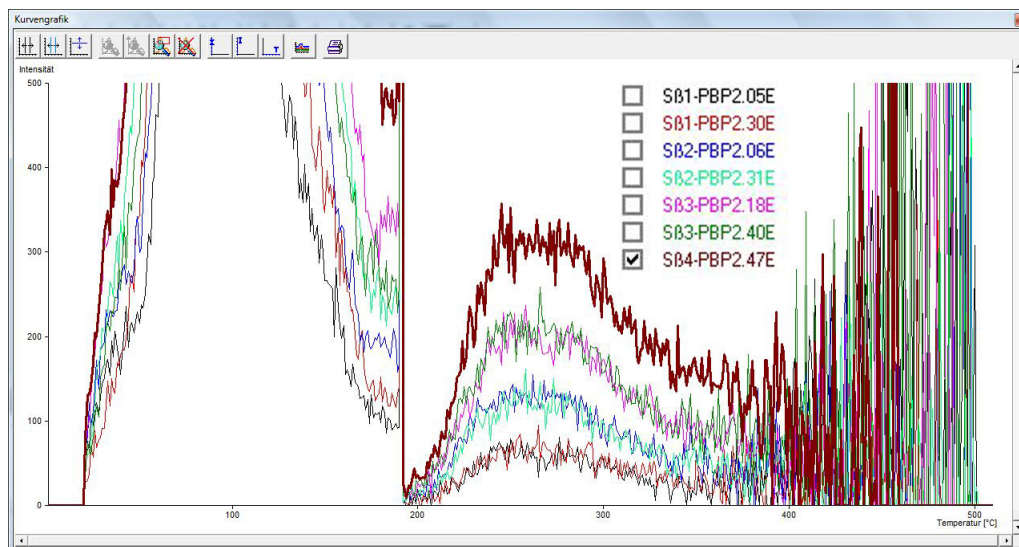


Figure 4.19: Second-glow-curves of sample “PBP2”

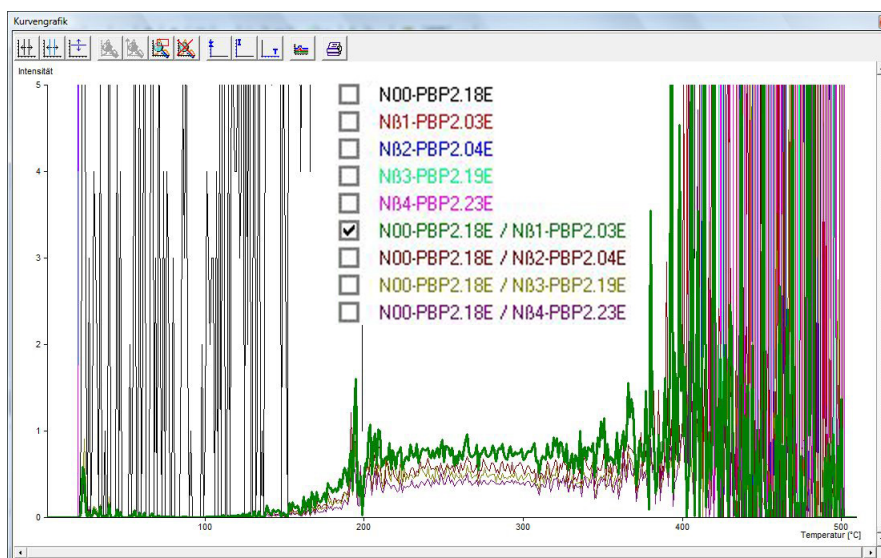


Figure 4.20: Plateau of sample “PBP2”

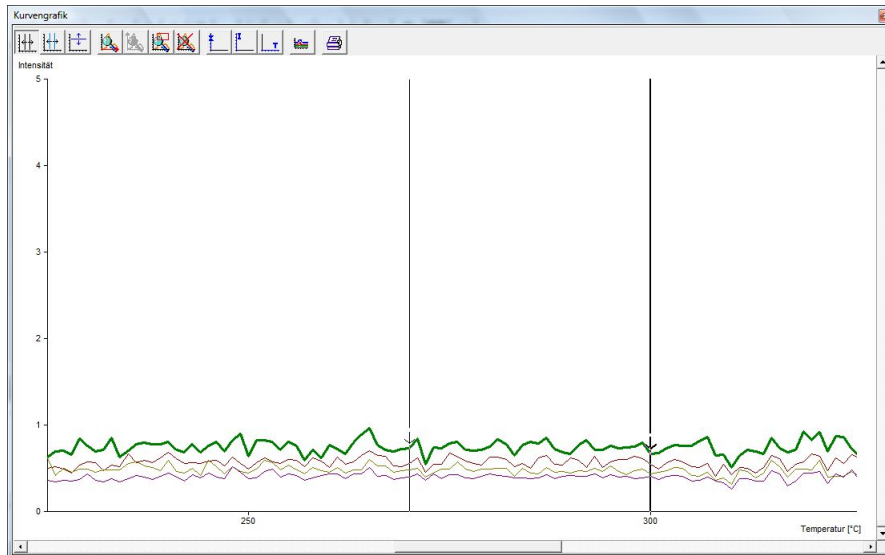


Figure 4.21: Plateau test with zoomed integration interval (270-300 °C) of sample “PBP2”

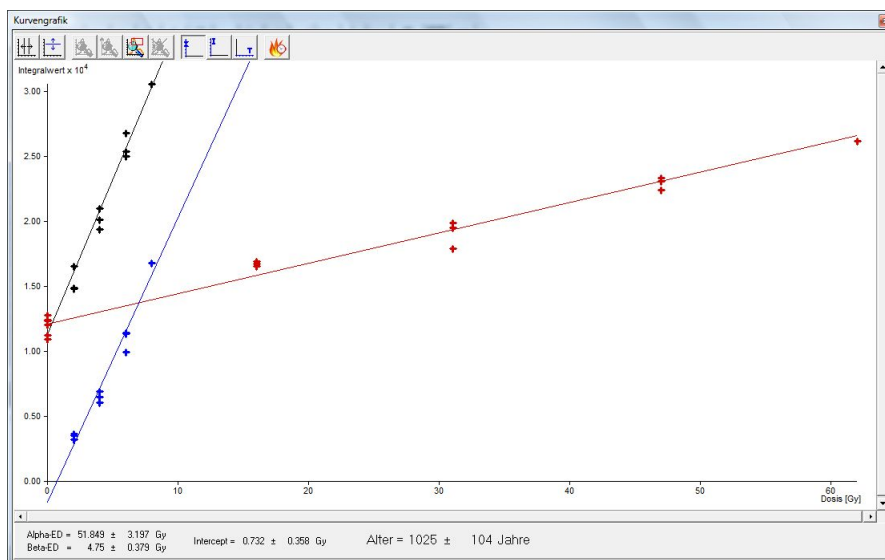


Figure 4.22: Regression lines of sample “PBP2”

The screenshot shows the 'Age Calculation' software window. The 'Measurement Technique' is set to 'Fine Grain Technique'. The 'Title' is 'Sample "PBP2"' and the 'Date of Measurement' is '21.10.2009'. The input parameters are as follows:

- $Q_\alpha$ : 37.856 ± 2.293 Gy
- $Q_\beta$ : 5.665 ± 0.268 Gy
- $I$ : 0.431 ± 0.351 Gy
- $A$ : 0.15 ± 0.002
- $\alpha$  - Counting Rate: 11.616 Counts/ks
- Pairs Rate: 0.257 Counts/ks
- Saturation Weight Increase: 0.22
- Saturation Fraction: 0.82 ± 0
- $K_2O$ -Contents: 2.93 Wt %
- $\beta$  - Attenuation: 1
- Internal  $\gamma$  - Dose-Rate ( $\dot{D}_{\gamma int}$ ): 1.366 mGy/a
- External  $\gamma$  - Dose-Rate ( $\dot{D}_{\gamma ext}$ ): 0.289 ± 0.050 mGy/a
- Sample Shape: flat
- Sample Thickness: 0.9 cm
- $p$ : 11.57 %
- Saturation Weight Increase of Soil: 0

The calculated results are shown on the right side of the window:

- Effective  $\alpha$  - Dose-Rate ( $\dot{D}'_\alpha$ ): 1.747 mGy/a 36.79 %
- $\beta$  - Dose-Rate ( $\dot{D}_\beta$ ): 2.412 mGy/a 50.79 %
- $\gamma$  - Dose-Rate ( $\dot{D}_\gamma$ ): 0.414 mGy/a 8.72 %
- Cosmic Dose-Rate ( $\dot{D}_c$ ): 0.176 mGy/a 3.71 %
- Total Dose-Rate ( $\dot{D}$ ): 4.749 mGy/a
- TL Measurement: 6.72 %
- Annual Dose: 3.28 %
- Stone Content: 0 %
- Error Stone Content
- Total Random Error: 7.48 %
- Calibration: 4.91 %
- Th/U-Ratio: 0 %
- Wetness: 0 %
- Total Systematic Error: 4.91 %
- Total Error: 8.95 %
- Age: 1284 ± 115 Years (725 a.c.)

The bottom of the window contains buttons for OK, Execute, Cancel, Load, Save, Print, Default Values, E, DE, and Help.

Figure 4.23: Age Calculation of sample “PBP2”

### Determined parameters (see section 3.1):

- $\alpha$ -counting rate [Counts/ks]: 11.616; Pairs rate [Counts/ks]: 0.257
- Saturation weight increase: 0.22; Saturation fraction: 0.82
- $K_2O$ -contents [%]: 2.93; was determined by measuring the sample along with two standard materials, the average value was taken
- External  $\gamma$ -dose rate [mGy/a]: 0.289 (Tschirf et al., 1970) [23]
- Cosmic dose rate [mGy/a]: 0.176

## 5 Conclusion

In this thesis the age determination via thermoluminescence of two samples has been accomplished. One is a brick from Alkoven in Upper Austria and the other one is a fragment excavated in Petronell-Carnuntum in Lower Austria. The fine-grain technique has been used for both samples.

Furthermore, a program module of the dating software used at the Institute of Atomic and Subatomic Physics of Vienna University of Technology has been renewed and enhanced. The analysis of the sample “PBP1” was made with both the original and the enhanced software version so as to check and confirm the equivalence of both.

By drilling enough sample powder was gained, the fractionation and sedimentation were accomplished without any difficulties and there was an adequate amount of coated disks which could be used for further measuring. The data was then analyzed using the dating software mentioned above.

In order to obtain the most accurate age of the samples, parameters essential for the age determination ( $\alpha$ -counting rate, potassium-oxide concentration, external  $\gamma$ -dose rate, cosmic dose rate, etc.) were ascertained.

### 5.1 Sample of Alkoven, “PBP1”

A successful age determination of this sample was accomplished:  $1025 \pm 104$  years (984 a. c.) As a result the origin of the sample dates back to the end of the early Middle Ages. The errors add up to approximately 10 % which is acceptable.

Parameters were determined as follows:

- $\alpha$ -counting rate [Counts/ks]: 16.561
- Pairsrate [Counts/ks]: 0.33
- $K_2O$ -contents [%]: 3.29
- External  $\gamma$ -dose rate [mGy/a]: 0.327
- Cosmic dose rate [mGy/a]: 0.177

## 5.2 Sample of Petronell-Carnuntum, “PBP2”



This sample with its  $1284 \pm 115$  years dates back to the early Middle Ages as well. The total error is 8.95 % which is satisfying.

The determined parameters for this sample are:

- $\alpha$ -counting rate [Counts/ks]: 11.616
- Pairsrate [Counts/ks]: 0.257
- Saturation weight increase: 0.22
- Saturation fraction: 0.82
- $K_2O$ -contents [%]: 2.93
- External  $\gamma$ -dose rate [mGy/a]: 0.289
- Cosmic dose rate [mGy/a]: 0.17



## A Printout of Sample “PBP2”

	TECHNISCHE UNIVERSITÄT WIEN VIENNA UNIVERSITY OF TECHNOLOGY Stadionallee 2, 1020 Wien, AUSTRIA	ATOMINSTITUT DER ÖSTERREICHISCHEN UNIVERSITÄTEN ATOMIC INSTITUTE OF THE AUSTRIAN UNIVERSITIES www.ozi.ac.at	
---	--	---	---

**Sample "PBP2"**

Excavation Site: Petronell-Carnuntum  
Sea Level of Excavation Site [m]: 175  
Geographical Position: 48° 7' N, 16° 51' E  
Date of Measurement: 21.10.2009

---

Alpha-Equivalent Dose:	37,856 +/- 2,293	Gy
Beta-Equivalent Dose:	5,665 +/- 0,268	Gy
Intercept:	0,431 +/- 0,351	Gy
Paleodose:	6,096 +/- 0,619	Gy
Alpha-Effectiveness:	0,15 +/- 0,002	Gy

Alpha-Dose-Rate:	1,747	mGy/a
Beta-Dose-Rate:	2,412	mGy/a
Gamma-Dose-Rate:	0,414	mGy/a
Cosmic Dose-Rate:	0,176	mGy/a

---

Total Dose-Rate:	4,749	mGy/a
------------------	-------	-------

**Age 1284 +/- 115 Years**  
[725 a.c.]

---

1

Figure A.1: Printout of sample “PBP2”, page 1

Alpha-Counting Rate:	11,616	Counts/ks
Pairs Rate:	0,257	Counts/ks
Saturation Weight Increase:	0,22	
Saturation Fraction:	0,82 +/- 0	
Potassium Oxide-Contents:	2,93 Wt %	
Beta-Attenuation:	1	
Internal Gamma-Dose-Rate:	1,366	mGy/a
External Gamma-Dose-Rate:	0,289 +/- 0,050	mGy/a
Sample Shape:	flat	
Sample Thickness:	0,9 cm	
Self-Dose Factor:	11,57 %	
Saturation Weight Increase of Soil:	0	

#### Errors

TL Measurement:	6,72	%	Calibration:	4,91	%
Annual Dose:	3,28	%	Th/U-Ratio:	0	%
Stone Content:	0	%	Wetness:	0	%
Total Random Error:	7,48	%	Total Systematic Error:	4,91	%

Total Error: 8,95 %

Figure A.2: Printout of sample "PBP2", page 2

## References

- [1] R. Chen and S. W. S. McKeever, *Theory of Thermoluminescence and Related Phenomena*. World Scientific Publishing, 1997.
- [2] M. J. Aitken, *Thermoluminescence Dating*. Academic Press, 1985.
- [3] L. Bøtter-Jensen, *Luminescence techniques: instrumentation and methods*, *Radiation Measurements* **27**, No. 5/6 (1997) 749–768.
- [4] J. Bruce, R. B. Galloway, H. K., and E. Spink, *Bleaching and phototransfer of thermoluminescence in limestone*, *Radiation Measurements* **30** (1999) 497–504.
- [5] M. J. Aitken, *An Introduction to Optical Dating: The Dating of Quaternary Sediments by the Use of Photon-stimulated Luminescence*. Oxford University Press, 1998.
- [6] J. R. Prescott and L. G. Stephan, *The contribution of cosmic radiation to the environmental dose for thermoluminescent dating: Latitude, altitude and depth dependences*, *PACT* **6** (1982) 17–25.
- [7] H. Tatlisu, *Sediment dating by thermoluminescence and optical stimulated luminescence*, Master’s thesis, TU Wien, 2004.
- [8] S. W. S. McKeever, *Thermoluminescence of solids*. Cambridge University Press, 1985.
- [9] P. J. Mohr, B. N. Taylor, and D. B. Newell, *CODATA Recommended Values of the Fundamental Physical Constants: 2006*, *Rev. Mod. Phys.* **80** (2008) 633–730.
- [10] S. W. S. McKeever and R. Chen, *Luminescence Models*, *Radiation Measurements* **27**, No. 5/6 (1997) 625–661.
- [11] S. Basun, G. F. Imbusch, D. D. Jia, and W. M. Yen, *The analysis of thermoluminescence glow curves*, *Journal of Luminescence* **104** (2003) 283–294.
- [12] N. S. Rawat, M. S. Kulkarni, D. R. Mishra, B. C. Bhatt, C. M. Sunta, S. K. Gupta, and D. N. Sharma, *Use of initial rise method to analyze a general-order kinetic thermoluminescence glow curve*, *Nuclear Instruments and Methods in Physics Research B* **267** (2009) 3475–3479.

- [13] B. Li and S. H. Li, *Investigations of the dose-dependent anomalous fading rate of feldspar from sediments*, *J. Phys. D: Appl. Phys.* **41** (2008) 225502 (15pp).
- [14] I. Jaek, A. Molodkov, and V. Vasilchenko, *Possible reasons for anomalous fading in alkali feldspars used for luminescence dating of Quaternary deposits*, *Estonian Journal of Earth Sciences* **56** (2007) 167–178.
- [15] A. Zink, *Uncertainties on the luminescence ages and anomalous fading*, *Geochronometria* **47-5032** (2008) 47–50.
- [16] A. Larsen, S. Greulich, M. Jain, and A. S. Murray, *Developing a numerical simulation for fading in feldspar*, *Radiation Measurements* **44** (2009) 467–471.
- [17] W. Gratzl, *EDV-unterstützte Untersuchung des Einflusses des Thorium- und Urangehalts archäologischer Proben auf deren Thermolumineszenzdatierung*, Master's thesis, TU Wien, 1989.
- [18] R. Bergmann, *Vergleichende Untersuchungen der optisch stimulierten Lumineszenz und der Thermolumineszenz von Keramiken zum Zweck der Altersbestimmung*, Master's thesis, TU Wien, 2005.
- [19] S. M. Hossain, F. De Corte, D. Vandenberghe, and P. Van den haute, *A comparison of methods for the annual radiation dose determination in the luminescence dating of loess sediment*, *Nuclear Instruments and Methods in Physics Research Section A: Accelerators, Spectrometers, Detectors and Associated Equipment* **490** (2002) 598–613.
- [20] I. Liritzis, *Advances in thermo- and opto-luminescence dating of environmental materials (Sedimentary Deposits) part I: technique*, *Global Nest: the International Journal* **2, No. 1** (2000) 3–27.
- [21] W. Primerano, *Thermolumineszenzdatierung von archäologischen Funden aus dem Mittelneolithikum, Bronzezeit und der römischen Kaiserzeit*, Master's thesis, TU Wien, 1999.
- [22] R. C. Henzinger, *Entwicklung einer vollautomatischen Thermolumineszenz-Auswertanlage und ihre Anwendung in Dosimetrie und Archäometrie*. PhD thesis, TU Wien, 1993.
- [23] E. Tschirf, W. Baumann, R. Niesner, and P. Vychytil, *Strahlenkarte Österreichs - mittlere Bevölkerungsdosen im Freien durch terrestrische u. kosmische Strahlung*. Bundesministerium für Gesundheit und Umweltschutz, 1975.